Copy No. 111

RM No. A7L02

CONFIDENTIAL

RESEARCH MEMORANDUM

A SUMMARY AND ANALYSIS OF WIND-TUNNEL DATA ON THE LIFT AND HINGE-MOMENT CHARACTERISTICS OF CONTROL SURFACES UP TO A MACH NUMBER OF 0.90

By John A. Axelson

Ames Aeronautical Laboratory,
Moffett Field, Calif.

NATIONAL ADVISORY COMMITTEE FOR AERONAUTICS

WASHINGTON

April 30, 1948

CONFIDENTIAL

NATIONAL ADVISORY COMMITTEE FOR AERONAUTICS

RESEARCH MEMORANDUM

A SUMMARY AND ANALYSIS OF WIND-TUNNEL DATA ON THE LIFT AND HINGE-MOMENT CHARACTERISTICS OF CONTROL SURFACES UP TO A MACH NUMBER OF 0.90

By John A. Axelson

SUMMARY

An extensive collection of the lift and hinge-moment characteristics of control surfaces up to a Mach number of 0.90 has been assembled from high-speed wind-tunnel data. It covers a wide variety of control-surface profiles, plan forms and aerodynamic balances. The various factors which affect C_{L_α}, C_{L_δ}, C_{h_α}, and C_{h_δ} at high Mach numbers are discussed and the importance of control-surface profile on lift and hinge moments is stressed. This report should find wide application in control-surface design and control estimates.

INTRODUCTION

Considerable control-surface research has been conducted during the past decade and many attempts have been made to derive theoretical and empirical relations which will permit the aerodynamicist to predict control-surface characteristics with a reasonable degree of accuracy. The bulk of this effort and the major part of the available information, however, has been concerned with the low-speed, incompressible characteristics of control surfaces. (See references 1 through 8.) An urgent need exists for dependable information which can be used in the design of control surfaces for use at high speed. There have been repeated instances where control surfaces satisfactory for low-speed use were unsuitable for high-speed use.

Because of the large number of factors involved, prediction of control-surface characteristics at high speed is often more difficult than the prediction of the characteristics of a wing. The lack of a suitable theory accounting for the effects of compressibility, separation, gap, surface discontinuities, and

many other variables affecting control-surface characteristics has resulted in the widespread use of experimental data as the best guide. Unfortunately, most high-speed wind-tunnel investigations conducted during the past few years were directed toward the development or improvement of specific tactical airplanes and systematic high-speed control-surface research has been initiated only recently. The present report combines the extensive high-speed control-surface data obtained from many unrelated investigations with more recently obtained results and includes a discussion of the general high-speed control problems.

SYMBOLS

C_h control surface hinge-moment coefficient $\left(\frac{\text{hinge moment}}{qb_f\overline{c_f^2}}\right)$

C_L lift coefficient $\left(\frac{\text{lift}}{qS}\right)$

C_l rolling-moment coefficient $\left(\frac{\text{rolling moment}}{qSb}\right)$

q free-stream dynamic pressure $(\frac{1}{2}\rho V^2)$, pounds per square foot

ρ free-stream mass density, slugs per cubic foot

V free-stream velocity, feet per second

S surface area, square feet

b span perpendicular to plane of symmetry, feet

b_f span of control surface along hinge line, feet

l distance from centroid of tab to control-surface hinge line, feet

c local chord, feet

$\overline{c_f^2}$ root mean squared chord of control surface normal to the hinge line, feet

c_b chord of nose overhang forward of hinge line, feet

α angle of attack, degrees

δ control-surface deflection in a plane perpendicular to the hinge line, degrees

M free-stream Mach number

c_{L_α} $\left(\frac{\partial c_L}{\partial \alpha}\right)_{M,\delta}$

c_{L_δ} $\left(\frac{\partial c_L}{\partial \delta}\right)_{M,\alpha}$

c_{h_α} $\left(\frac{\partial c_h}{\partial \alpha}\right)_{M,\delta}$

c_{h_δ} $\left(\frac{\partial c_h}{\partial \delta}\right)_{M,\alpha}$

φ_1 included angle at the trailing edge between tangents to the control-surface profile, degrees (See fig. 3.)

φ_2 included angle between lines through the trailing edge to the upper and lower surfaces at the hinge line, degrees (See fig. 3.)

r ratio of the included angle at the trailing edge between tangents to the control-surface contour to the trailing-edge angle of a corresponding flat-sided control surface, (φ_1/φ_2).

Subscripts

f control surface

t tab

REDUCTION AND PRESENTATION OF RESULTS

A collection of high-speed wind-tunnel data on control surfaces is presented in this report. It covers a wide selection of plan forms, airfoil sections, aerodynamic balances, and control-surface profiles. A list of the control surfaces and the important aerodynamic dimensional data is presented in table I. For simplicity, each control surface and tab for which data are presented is designated by a letter. The plan forms and section profiles of the control surfaces are shown in figure 1. Duplication of results has been avoided in cases were two or more wind-tunnel investigations covered control surfaces of nearly identical

dimensions and characteristics. In such cases, only the control surface for which the highest test Mach number was attained has been included in this analysis. Control surface X was tested in the Langley 16-foot high-speed wind tunnel and the others listed in table I were tested in the Ames 16-foot high-speed wind tunnel.

Since most of the control surfaces were tested as integral parts of complete airplane models, no accurate determination of the drag characteristics was made. Further, insufficient pressure-distribution measurements were obtained to permit a detailed study of the pressures. Therefore, only the lift and hinge-moment characteristics have been included in this report. There were insufficient high-speed data on tab hinge moments to make an adequate comparison. The tab effectiveness, however, has been summarized for several different tab installations.

Tunnel-wall and constriction corrections have been applied to the results wherever the magnitude of the correction was large enough to be of importance. The Reynolds numbers for all tests were high enough to make the results generally applicable to full-scale design. At a Mach number of 0.3, the Reynolds number was 1.2×10^6 for the control surface G which was tested as the horizontal tail of a relatively small model of a complete airplane. In nearly all of the other tests the Reynolds number exceeded 2×10^6 at a Mach number of 0.3.

The hinge-moment characteristics of the control surfaces are presented in figures 2(a) to 2(y). Figure 3 presents sketches showing the manner in which the control-surface parameter r is evaluated for different control surfaces of varying profile. This parameter was found useful in comparing the results and is used in figure 4 which shows the variation of C_{h_α} and C_{h_δ} with Mach number for control surfaces having radius noses and a variety of profiles aft of the hinge line. Figure 5 presents the variations of C_{h_α} and C_{h_δ} with Mach number for control surfaces having overhang and internal nose balances. The variations of the lift parameters, C_{L_α} and C_{L_δ}, with Mach number for the control surfaces for which the data were available are presented in figure 6. Figure 7 shows the extent to which slight revisions in profile near the trailing edge affected the rolling effectiveness of control surfaces E and F. Figure 8 summarizes the variation of tab effectiveness with Mach number for several different control-surface combinations.

RESULTS AND DISCUSSION

Elevator Hinge Moments and Longitudinal Control

The majority of the control problems encountered with high-speed airplanes during the past several years have pertained to longitudinal stability and trim. The causes of and means for controlling the nosing-down tendency of airplanes at high speeds have been studied quite thoroughly and have been summarized in reference 9, which also includes an analysis of the influence of elevator hinge moments on the high-speed control.

Since the longitudinal stability and control of high-speed airplanes are vitally affected by changes in the wing lift-curve slope, angle of attack for zero lift, wing pitching-moment characteristics, wing span load distribution, and downwash in addition to the characteristics of the horizontal tail, it is difficult to formulate design criteria which will be applicable to all airplanes. However, there are several concepts dealing with the design of high-speed control surfaces which are generally applicable.

It is commonly known that as the size and speed of airplanes are increased, the loads on the surfaces are also increased. In order to keep the stick forces within the control of the pilot, aerodynamic balances, tabs, or boosts must be used in the control system. In choosing the aerodynamic balance, both C_{h_α} and C_{h_δ} must be considered. Although it is possible to obtain an acceptable variation of stick force with airplane normal acceleration which is independent of center-of-gravity location by combining zero C_{h_δ} and a slightly positive C_{h_α}, it is common to use a slightly negative C_{h_δ} to prevent rapid movement of the control surfaces and to avoid the possibility of over-balanced control surfaces and unstable stick-force gradients at high Mach numbers. Two factors control the selection of C_{h_α}; namely, control forces and center-of-gravity travel. A slightly negative C_{h_α} is usually desirable, but if a large travel is required for the center of gravity, it is generally necessary to use a positive C_{h_α} in order to move the stick-free neutral point aft of the stick-fixed neutral point. However, the stick-force gradient imposes a restriction on the amount of positive C_{h_α} which can be permitted, since a positive C_{h_α} tends to heavy the elevator hinge moments encountered in flight maneuvers.

A further restriction is imposed on the use of positive C_{h_α} at Mach numbers well above the critical of an airplane, where the use of an elevator exhibiting a large positive C_{h_α} generally leads to excessive pull forces at the controls. In this regard, the use of a thicker airfoil section at the root of the wing than at the tip and other factors such as interference effects of nacelles and fuselages tend to lower the critical Mach number of the inboard section of the wing. When the Mach number of lift divergence of the wing is exceeded, there results a reduction in the airplane lift-curve slope, an outboard shift in the wing span load distribution, and a reduction in the downwash on the tail. If the wing is cambered, there also occurs an increase in the wing angle of attack for zero lift. The reduced lift-curve slope and increased zero-lift angle increase the airplane angle of attack required for level flight. The net result of these adverse changes is a marked increase in the airplane static longitudinal stability and a sizeable increase in the angle of attack of the horizontal tail, requiring increasingly larger up-elevator deflections. If the airplane were equipped with elevators displaying a negative C_{h_δ} and positive C_{h_α}, the increase in tail angle of attack would be accompanied by further increases in the elevator hinge-moment coefficient. Excessive control forces generally result unless a trimming device, such as a dive recovery flap, is available and is effective at the high Mach number in question. A summary and analysis of data on dive-recovery flaps has already been presented in reference 10, no repetition of results being necessary in this report. Since the present analysis is primarily concerned with hinge moments, no results have been included for spoilers where the hinge moment is generally unimportant. Detailed data on spoilers may be found in references 11, 12, and 13.

Aileron Hinge Moments and Lateral Control

As in the case of elevators it is generally necessary to employ aerodynamic balance, a balance tab, a servotab, or some type of boost in the aileron system in order to keep stick forces within the pilot's control. At both low and high speeds, the magnitudes of the hinge moments of the ailerons are affected by wing camber, by the differences in the angles of attack of the wing tips during roll, and by the use of unequal up and down aileron deflections often used to obtain desirable yawing characteristics. There is also a possibility of adverse control tendencies accompanying aileron deflection with an airplane operating slightly above its critical Mach number, because deflection of the ailerons changes the critical Mach numbers of the wing tips and may result in local shock-wave formation, separation, and reduced effectiveness of one or both ailerons.

To avoid the possibility of overbalancing of the ailerons at high Mach numbers, it is desirable to have a slightly negative C_{h_δ} throughout the expected operating range of Mach numbers and zero or slightly negative C_{h_α} in order to maintain light control forces over the desired range of angles of attack. A positive C_{h_α} tends to increase the hinge moments encountered in flight with ailerons displaying a negative C_{h_δ}, because of the variation in the angles of attack of the wing tips with rolling motion.

Control-Surface Characteristics

Sweep.— Control surfaces B, E, F, and G have swept-back plan forms for the purpose of increasing the Mach numbers of lift and hinge-moment divergence. The same model was used for the tests of control surfaces A and B except that the hinge lines were swept 0° and 45°, respectively. The flap in both cases was the simplest type, having a radius nose and flat sides. The complete data obtained from these tests are presented in reference 14.

As shown in figure 6, sweeping the model back reduced the lift-curve slope C_{L_α} to almost one-half the unswept value and decreased the flap effectiveness C_{L_δ} to less than one-third the unswept value below 0.80 Mach number; but it should be noted that the aspect ratio was reduced from 5.36 to 2.31. The reduction in C_{L_α} was in fair agreement with the general rule that the lift-curve slope is proportional to the cosine of the angle of sweep at small angles of attack. The large reduction in C_{L_δ} can be explained by the fact that the area of the swept model B was approximately 40 percent greater than that of the unswept model A, but the flaps were the same size. If the flap effectiveness of the two models be expressed in terms of an equal area, the ratio of the values of C_{L_δ} then approximates the cosine rule.

In the results shown in figure 6(a), the lift-curve slopes of the unswept control surfaces increase with Mach number up to the Mach number of lift divergence, the variation being well approximated by the three-dimensional Glauert factor which depends primarily on aspect ratio as discussed in reference 15. The increases in lift-curve slopes with Mach number for the swept surfaces B and G, however, are much more gradual, indicating that possibly the Mach number component perpendicular to the quarter-chord line should be used in computing the quantity $(1-M^2)$. The flap effectiveness parameter shown in figure 6(b) remains relatively constant with Mach number up to the Mach number of lift divergence for both the swept and unswept control surfaces.

As shown by the hinge-moment characteristics for control surfaces A and B in figures 2(a) and 2(b), sweeping the model reduced the variations of hinge-moment coefficient with control-surface deflection and with angle of attack. The reductions in C_{h_α} and C_{h_δ} accompanied the reduction in C_{L_δ}.

It might be mentioned that if the choice between swept and unswept horizontal tails was being considered for a given airplane, the area of the tail would have to be increased as the sweep was increased in order to provide the same amount of static longitudinal stability at low Mach numbers because of the reduction in tail-plane lift-curve slope with increasing sweep. For an airplane which is to fly at Mach numbers above 0.85, the use of sweep offers definite advantages by delaying the effects of compressibility on both lift and hinge moments to higher Mach numbers and by reducing the magnitude of the changes when they occur. In selecting the amount of sweep to be used, it is desirable to keep the sweep angle to a minimum in order to maintain high C_{L_α} and C_{L_δ} over the entire speed range. On the other hand, the gain in critical Mach number from the use of sweep is often only one-half that indicated by the cosine approximation because of interference at the plane of symmetry and separation resulting from the spanwise flow of air in the boundary layer induced by spanwise pressure gradients. The interference and separation can be reduced by proper contouring of the fuselage-wing or fuselage-stabilizer intersections and possibly by the use of boundary-layer control.

Airfoil section.- The choice of airfoil section for a high-speed wing or horizontal tail is governed in part by structural considerations and by the type of control surface to be used. If a relatively large nose balance is to be employed on the control surface, it is desirable to have sufficient thickness to allow ample deflection of the control surface without the nose balance projecting excessively. In the case of an internal nose balance, sufficient space is required within the profile to permit ample motion of the balance.

Locating the maximum thickness near the midchord satisfies the control-surface space requirements and allows a maximum depth for a centrally located spar. However, for airfoils with the maximum thickness relatively far aft on the chord, the greater adverse pressure gradient over the aft portion of the airfoil is conducive to separation at higher Mach numbers which tends to reduce the flap effectiveness. Such an effect is indicated by the flight-test results presented in reference 16 wherein the reduction in flap effectiveness started at a considerably lower Mach number and became more pronounced on a wing having an NACA 66-series airfoil than on

a similar wing having an NACA 230-series airfoil section. The same effect of separation is shown in reference 9 which includes some flap data from high-speed wind-tunnel tests of 20-percent chord flaps on airfoils having a NACA 65-210 section. Preliminary considerations of the dynamics of the air particles flowing at high speed over a control-surface combination indicate that discontinuities in the slope of the surface or in the rate of change of slope with chordwise distance aft of the maximum thickness strongly influence separation because of the vertical accelerations required of the air in following the profile. Although no systematic high-speed investigation has been conducted on the matter, existing data on flap effectiveness favor the more forward locations of maximum thickness and flat-sided surfaces. The matter is closely related to the control-surface profile and trailing-edge angle.

Camber affects the critical Mach number and the high-speed aerodynamic characteristics of airfoils as discussed in reference 9, but does not have any large effect on control-surface characteristics except for a slight change in the hinge-moment coefficient.

Favorable tail characteristics can be obtained up to a Mach number of at least 0.85 without resorting to the use of sweep by using reduced thickness-to-chord ratios. By comparing the results in figures 5 and 6, which present the variations of C_{h_α}, C_{h_δ}, C_{l_α}, and C_{l_δ} with Mach number for several control-surface combinations, it can be seen that control surface I, having NACA 0009- and 0007-airfoil sections at the root and tip, respectively, and having flat-sided elevators, exhibits no adverse characteristics up to a Mach number of 0.85, the limit of the test. Reference 9 contains extensive high-speed airfoil data on the effects of thickness. In using reduced thickness-to-chord ratios, locating the maximum thickness forward of the 40-percent chord line permits a larger leading-edge radius than could be used with more aft chordwise locations of maximum thickness.

Control-surface profile aft of the hinge line.- The importance of control-surface profile aft of the hinge line on the high-speed control-surface characteristics has been fully realized only recently. In many high-speed wind-tunnel and flight investigations, drastic changes in control-surface characteristics were unexpectedly encountered at high Mach numbers. In some cases, the unusual characteristics were found to be associated with bulges and in others with the trailing-edge angle of the control surface. Comparison of the control-surface profiles described in table I and

figure 1 with the hinge moments in figure 2 indicated that the parameter r, defined in the symbols and in figure 3, could be used to correlate the data for the various profiles. As shown in figure 4(a), the parameter r provides a fair index of the C_{h_α} of the various control surfaces in spite of the large differences in airfoil sections, thickness-to-chord ratios, critical Mach numbers, and plan forms. The results in figure 4(b) indicate that r and the trailing-edge angle do not provide sufficient information for predicting C_{h_δ}, because of the effects of sweep and the profile over the forward part of the control surface. However, the parameter r gives a very good indication of the changes in both C_{h_α} and C_{h_δ} with increasing Mach number. The results indicate that r should be kept near unity, and that the trailing-edge angle should be kept below 14°. The increasingly powerful balancing effect of beveled trailing edges at higher Mach numbers may be realized by comparing the hinge-moment characteristics of control surfaces J and K in figures 2(g) and 2(k) and by comparing those of central surfaces T and V in figures 2(t) and 2(v), respectively. In both cases, the addition of the bevels produced excessive overbalance at the higher Mach numbers, and also reduced the effectiveness of the control surfaces as shown in figure 6(b) for control surfaces J and K and in reference 17 for control surfaces T and V.

A strong indication of the reduction in control-surface effectiveness caused by an excessive trailing-edge angle is shown in figure 7 for the swept control surfaces E and F. The convex sides and the accompanying large trailing-edge angle greatly reduced the effectiveness of the control surface E at high Mach numbers. Flattening the sides by extending the chord as shown in figure 1(b) approximately doubled the effectiveness at 0.9 Mach number, as shown in figure 7. A corresponding improvement was obtained in the hinge-moment characteristics as shown in figures 2(e) and 2(f).

Further evidence of the manner in which trailing-edge profile affects control-surface characteristics is shown in figure 2(w) for the all movable surface W. In this case C_{h_α} and C_{h_δ} are essentially the same parameter and correspond to the pitching-moment characteristics of a wing of equal aspect ratio, plan form, and airfoil section. Although the hinge moments were measured about the 15-percent-chord line, both C_{h_α} and C_{h_δ} become increasingly positive with increasing Mach number, because of the large trailing-edge angle and convex profile of the NACA 16-009 airfoil section. High-speed data on low-aspect-ratio wings provide the best guide for predicting the characteristics of all-movable control surfaces.

Additional data on the effects of bevels and bulges on control-surface characteristics are presented in references 9 and 18. When using elliptical plan forms or curved trailing edges such as on control surface H, attention should be given to the maintenance of a uniformly small trailing-edge angle along the entire span of the control surface.

Nose balance.- Aerodynamic nose balances have been used extensively for reducing C_{h_δ} of control surfaces. The two common types of nose balance are the overhang type, such as employed on control surfaces H, I, J, K, L, M, N, Q, R, S, and X and the internal-balance type, used on control surfaces O, P, T, U, V, and Y. The hinge-moment characteristics of all of these control surfaces are presented in figure 2. Both C_{h_α} and C_{h_δ} evaluated at zero angle of attack and zero control-surface setting are summarized in figure 5. Control surfaces O, P, and U, having internal balances, are marked with asterisks to identify them from the rest of the control surfaces which have simple overhang balances.

Figure 5(a) indicates that there is relatively little variation in C_{h_α} with length of overhang for control surfaces having flat sides; but when the thickness of the overhang is greater than that at the hinge line, C_{h_α} tends to be positive, as shown for control surfaces X and N. Control surface S, which is essentially control surface Q with a horn balance attached, exhibits the markedly positive C_{h_α} of 0.007; while control surface U, which has concave sides and a sealed, internal balance, exhibits a strongly negative C_{h_α}. Control surface K, having the beveled trailing edge but the same plan form and nose balance as control surface J, exhibits marked overbalance at the higher Mach numbers, as shown in figure 2(k). The balancing effects of the nose balance and the beveled trailing edge are additive. Because of the large positive C_{h_δ}, control surface K is not suitable for high-speed use. In general, the results indicate that aerodynamic balances can be used effectively up to a Mach number of at least 0.85 and probably higher, provided the nose shape is properly formed and the thickness-to-chord ratio and trailing-edge angle are kept sufficiently small.

Means for controlling C_{h_α} and C_{h_δ}.- The results in figures 2, 4, and 5 indicate that the profile of the control surface aft of the hinge line greatly influences C_{h_α} and C_{h_δ}. A bulged or beveled profile ($r > 1$) tends to produce positive C_{h_α} and C_{h_δ}, the effect becoming more pronounced with increasing Mach number. Flat-sided ($r = 1$) or cusped profiles ($r < 1$) generally produce negative C_{h_α}

and C_{h_δ}. Exposed or unshielded horn balances provide an effective means for increasing C_{h_α} and C_{h_δ} as shown in figures 2(s) and 5. The lack of symmetry in the hinge moments of figures 2(r) and 2(s) were caused by deformation of the model which was part of a prototype airplane and did not possess the rigidity of specially constructed high-speed wind-tunnel models. Reference 19 presents additional results and discussion of shielded and unshielded horn balances and covers several control-surface combinations, including Q, R, and S. Trailing-edge strips or beads are effective in making C_{h_α} and C_{h_δ} more negative, as shown in reference 20 which covers tests of 1/16-inch-and 1/8-inch-diameter tubing fastened to the trailing edge of control surface X and tested at 0.35 Mach number. The effect of such trailing-edge strips is to alter the air flow over the control surface in such a manner that the streamlines resemble those over a cusped surface ($r < 1$). Aerodynamic nose balances are effective in controlling C_{h_δ}, but as the thickness of the nose balance increases, C_{h_α} tends to increase positively.

Although C_{h_α} and C_{h_δ} are the most widely used hinge-moment parameters in control-surface studies, it should be remembered that the hinge-moment curve defined by the locus of points actually encountered in flight determines the control forces which will result. Thus, maneuvers are not conducted at constant angle of attack or at constant control-surface setting in the manner that C_{h_α} and C_{h_δ} are evaluated. Both α and δ change and it may readily be seen that the control forces depend on the combination of C_{h_α} and C_{h_δ}.

Tabs.- Because of the difficulty of measuring tab characteristics on small, high-speed wind-tunnel models, there is only a relatively small amount of data available. The variation of tab effectiveness with Mach number for six representative models is shown in figure 8. The area moment of a tab about the flap hinge line was suggested in reference 1 as a fair index of low-speed tab effectiveness. Dimensional parameters expressing the area moments of the tabs and ratio of tab area to flap area have been added to figure 8 in order to permit comparisons of the effectiveness of the various tabs. Neither parameter, however, accounts for the effects of boundary layer, separation, or leakage around the tab, all of which have a sizeable influence on the load on the tab.

The existing tab data indicate that the tab effectiveness decreases at the higher Mach numbers in a manner similar to the reduction in C_{L_δ} for the control surface. It might be expected then, that any contributing factor which causes separation and tends to decrease flap effectiveness at higher Mach numbers would

similarly affect the tab effectiveness. Beveled trailing edges, bulges, and convex sides, which were shown to have adverse effects on control-surface characteristics at high Mach numbers, would be expected to have detrimental effects on the tab characteristics.

No tab hinge moments have been summarized in this report because of the lack of sufficient high-speed data. Not only are tab hinge moments rather difficult to measure on small wind-tunnel models but, in most cases, the tab hinge moments have not been of primary importance to the aerodynamicist. Low-speed tab data may be found in references 1, 2, and 21. High-speed data on tab effectiveness are presented in references 11 and 22.

Transonic Flutter

In the design of high-speed control-surface installations, particular consideration should be given to the prevention of transonic flutter. It is not within the scope of this report to present a detailed analysis of transonic flutter. However, it is appropriate to mention that the phenomenon generally occurs at supercritical speeds in the presence of shock waves and is associated with the time lag between control-surface movement and the resulting changes in circulation and boundary layer. The rigidity, inertia, and aerodynamic balance of the control system are among the principal variables which may be used in controlling the flutter since they affect the natural frequency, the actuating forces, and the restraining forces on the control surface. Forthcoming publications on current flutter research should be consulted for further information.

CONCLUSIONS

From a summary and analysis of high-speed wind-tunnel data on control surfaces, the following conclusions are made concerning control-surface characteristics up to a Mach number of 0.90:

1. The adverse effects of compressibility on control-surface characteristics can be greatly reduced by using low thickness-to-chord ratios, locating the maximum thickness forward of the 40-percent chord line, maintaining minimum curvature and minimum changes of curvature aft of the midchord, and using flat-sided control surfaces having small trailing-edge angles.

2. Convex sides, bulges, bevels, and excessive trailing-edge angles on control surfaces tend to reduce the control-surface effectiveness and to increase the variations of C_{h_δ} and C_{h_α}

with Mach number, C_{h_δ} generally becoming unstable (positive) and C_{h_α} becoming increasingly positive up to the Mach number of lift divergence.

3. Concave or cusped sides on control surfaces tend to heavy the controls by making C_{h_δ} increasingly negative up to the Mach number of lift divergence.

4. The lift-curve slope C_{L_α} of control-surface combinations generally increases with Mach number up to the Mach number of lift divergence in a manner closely approximated by the three-dimensional Glauert factor.

5. The control-surface effectiveness C_{L_δ} generally remains essentially constant over the Mach number range below that for lift divergence for control surfaces having trailing-edge angles less than 14°. As the convexity and trailing-edge angle are increased, however, the control-surface effectiveness tends to decrease with increasing Mach number.

Ames Aeronautical Laboratory,
National Advisory Committee for Aeronautics,
Moffett Field, Calif.

REFERENCES

1. Goett, Harry J., and Reeder, J. P.: Effects of Elevator Nose Shape, Gap, Balance, and Tabs on the Aerodynamic Characteristics of a Horizontal Tail Surface. NACA Rep. No. 675, 1939.

2. Ames, Milton B. Jr., and Sears, Richard I.: Determination of Control-Surface Characteristics from NACA Plain-Flap and Tab Data. NACA Rep. No. 721, 1941.

3. Sears, Richard I.: Wind-Tunnel Data on the Aerodynamic Characteristics of Airplane Control Surfaces. NACA ACR No. 3L08, 1943.

4. Rogallo, F. M.: Collection of Balanced-Aileron Test Data. NACA ACR No. 4A11, 1944.

5. Purser, Paul E., and Toll, Thomas A.: Analysis of Available Data on Control Surfaces Having Plain-Overhang and Frise Balances. NACA ACR No. L4E13, 1944.

6. Swanson, Robert S., and Crandall, Stewart M.: Analysis of Available Data on the Effectiveness of Ailerons without Exposed Overhang Balance. NACA ACR No. L4E01, 1944.

7. Toll, Thomas A.: Summary of Lateral-Control Research. NACA TN No. 1245, 1947.

8. Root, L. E.: The Effective Use of Aerodynamic Balance on Control Surfaces. Jour. Aero. Sci., vol. 12, no. 2, Apr. 1945, pp. 149-163.

9. Axelson, John A.: Longitudinal Stability and Control of High-Speed Airplanes with Particular Reference to Dive Recovery. NACA RM No. A7C24, 1947.

10. Boddy, Lee E., and Williams, Walter C.: A Summary and Analysis of Data on Dive-Recovery Flaps. NACA RM No. A7F09, 1947.

11. Boddy, Lee E.: The High-Speed Characteristics of Several Flaps and Spoilers on the Upper Surface of the Horizontal Stabilizer of a 0.3-Scale Model of the Republic P-47D Airplane. NACA MR No. A5L07, 1946.

12. Laitone, Edmund V., and Summers, James: An Additional Investigation of the High-Speed Lateral-Control Characteristics of Spoilers, NACA ACR No. 5D28, 1945.

13. Spahr, J. Richard: Lateral-Control Characteristics of Various Spoiler Arrangements as Measured in Flight. NACA TN No. 1123, 1947.

14. Anderson, Joseph L., and Martin, Andrew: High-Speed Aerodynamic Characteristics of a Model Tail Plane with Modified NACA 65-010 Section and 0° and 45° Sweepback. NACA RM No. A7J22, 1947.

15. Axelson, John A., and Crown, J. Conrad: An Analysis of the Effects of Wing Aspect Ratio and Tail Location on Static Longitudinal Stability Below the Mach Number of Lift Divergence. NACA RM No. A7J13, 1947.

16. White, Maurice D., Sadoff, Melvin, Clousing, Lawrence A., and Cooper, George E.: Preliminary Results of a Flight Investigation to Determine the Effect of Negative Flap Deflection on High-Speed Longitudinal-Control Characteristics. NACA RM No. A7I26, 1947.

17. Laitone, Edmund V.: An Investigation of 0.15-Chord Ailerons on a Low-Drag Tapered Wing at High Speeds. NACA ACR No. 4I25, 1944.

18. Hall, Charles F.: The Effect of Modifications to the Horizontal-Tail Profile on the High-Speed Longitudinal Control of a Pursuit Airplane. NACA TN No. 1302, 1947.

19. Cleary, Joseph W. and Krumm, Walter J.: High-Speed Aerodynamic Characteristics of Horn and Overhang Balances on a Full-Scale Elevator. NACA RM No. A7H29, 1947.

20. Schueller, Carl F., Korycinski, Peter F., and Strass, H. Kurt: Tests of a Full-Scale Horizontal Tail Surface in the Langley 16-foot High-Speed Tunnel. NACA TN No. 1074, 1946.

21. Purser, Paul E., and Cook, Charles B.: Collection and Analysis of Hinge-Moment Data on Control-Surface Tabs. NACA TN No. 1113, 1947.

22. Erickson, Albert L., and Nelson, Warren H.: High-Speed Wind-Tunnel Tests of Semispan Horizontal Tails of the XB-42 Airplane with Fabric-Covered and Metal-Covered Elevators. NACA MR No. A4L18, 1944.

TABLE I.- AERODYNAMIC DIMENSIONAL DATA

Control surface	Airfoil section		Control surface contour	Average trailing-edge angle	Aspect ratio	Aerodynamic balance
	Root	Tip				
A	Modified NACA 65-010		Flat	12°	5.36	None
B			Flat	12°	2.31	None
C			Bulged	16°	4.81	Bulge
D	Modified NACA 0010		Bulged	12°	4.14	Bulge
E	NACA 0012-64	NACA 0011-64	Airfoil (convex)	20°	5.02	None
F	Modified NACA 0012-64 Extended Chord	NACA 0011-64	Flat	14°	4.79	None
G	NACA 0010-64		Airfoil (convex)	18°	4.65	None
H	Modified NACA 0009		Airfoil (convex)	12°	4.65	0.25 c_f overhang
I	NACA 0009	NACA 0007	Flat	10°	4.13	0.27 c_f overhang
J	NACA 0012	NACA 0009	Flat	13°	3.84	0.35 c_f overhang
K			Beveled	25°	3.84	0.35 c_f overhang, beveled trailing edge
L	NACA 65-011		Flat	14°	5.07	0.35 c_f overhang

TABLE I.- CONCLUDED.

Control surface	Airfoil section Root	Airfoil section Tip	Control surface contour	Average trailing-edge angle	Aspect ratio	Aerodynamic balance
M	B-117 t/c=0.19	B-117 t/c=0.09	Airfoil (concave)	13°	6.9	0.41 c_f overhang
N	Modified NACA 0012		Flat	14°	5.55	0.46 c_f overhang
O	NACA 65-213		Flat	16°	6.0	0.46 c_f sealed internal balance
P	NACA 65-015		Flat	17.5°	4.43	0.47 c_f sealed internal balance
Q	Modified NACA 0012-64 t/c=0.107		Flat	12°	3.67	0.33 c_f overhang
R			Flat	12°	4.43	0.33 c_f sealed overhang, shielded horn
S			Flat	12°	4.43	0.33 c_f sealed overhang, horn
T	NACA 66, 2-118	NACA 66, 2-116	Airfoil (concave)	13°	6.28	0.45 c_f sealed, internal balance
U			Airfoil (concave)	13°	6.28	0.60 c_f sealed, internal balance
V			Beveled	30°	6.28	0.42 c_f sealed, internal balance, beveled trailing-edge
W	NACA 16-009		Airfoil (convex)	24°	1.5	All-movable surface hinge at 0.15 chord
X	NACA 66-009		Flat	13°	4.76	0.48 c_f overhang
Y	B-117 t/c=0.20		Flat	22°	5.55	0.66 c_f internal balance

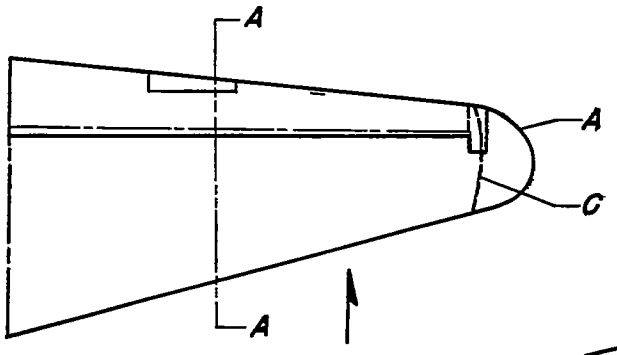

Planforms

Control Surfaces A and C

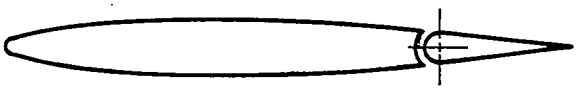

Section A-A

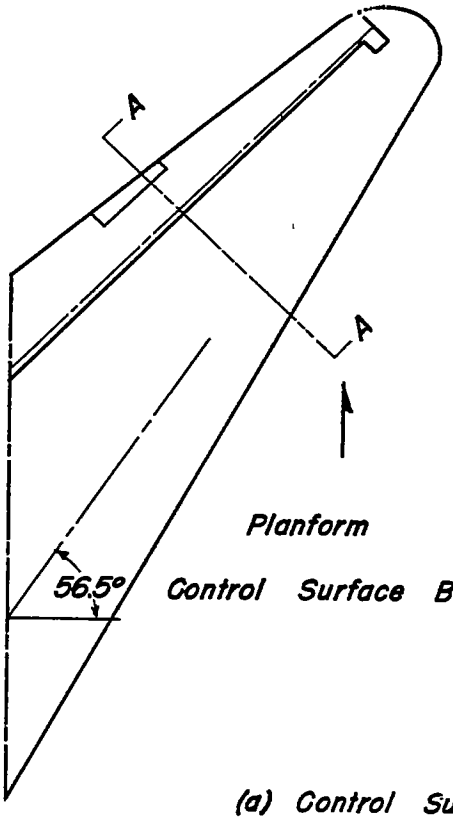

Planform

Control Surface B

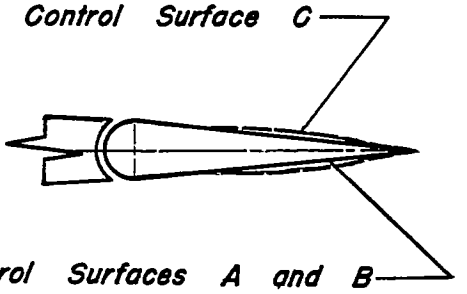

(a) Control Surface A, B, and C

Figure 1.— Planforms and section profiles of control surfaces.

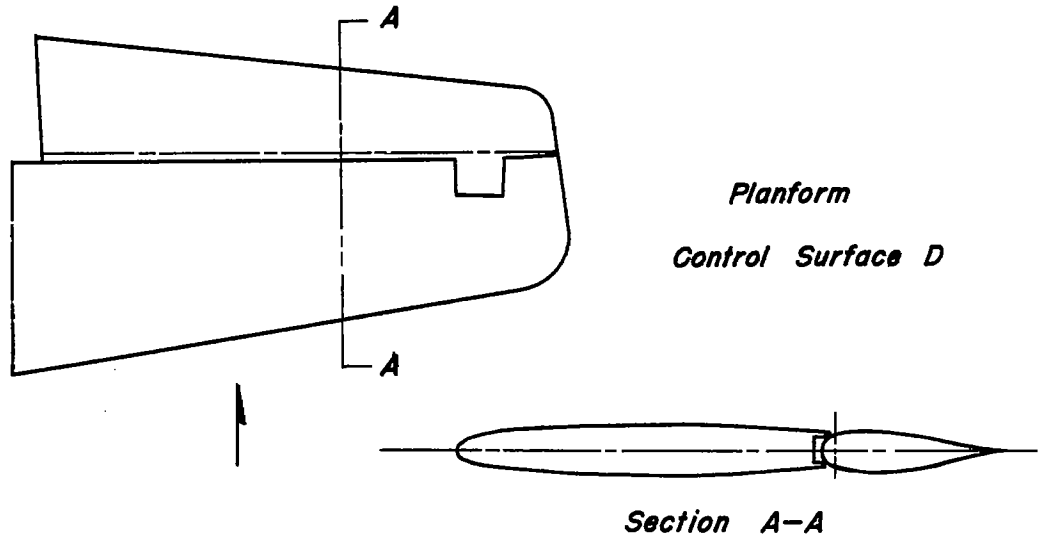

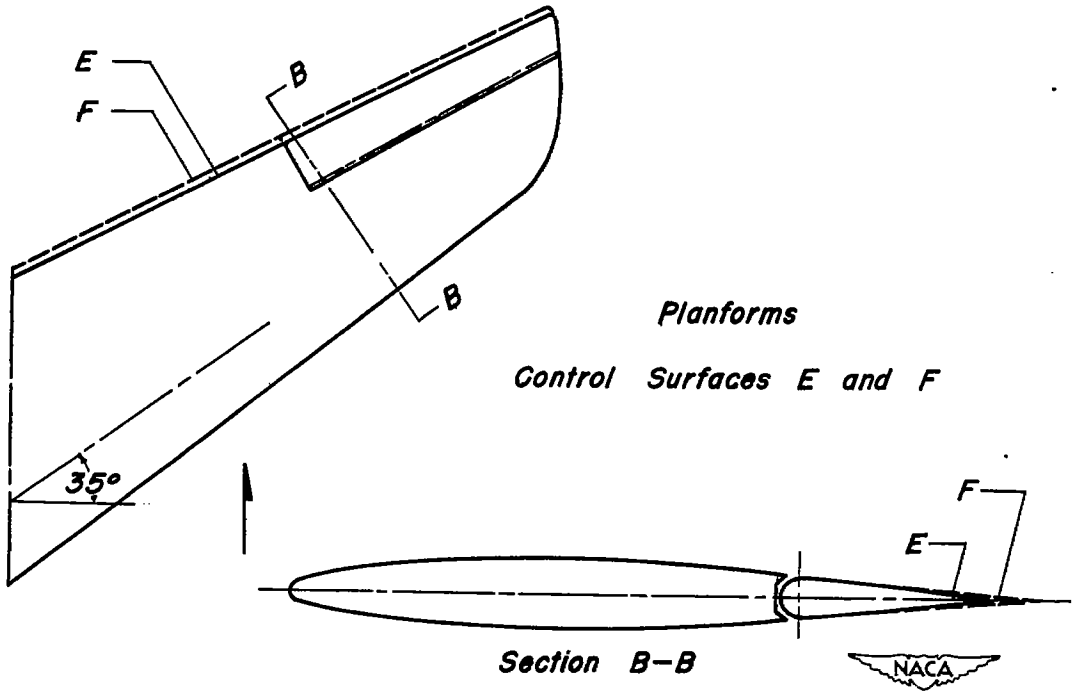

(b) Control Surfaces D, E, and F.

Figure 1.– Continued.

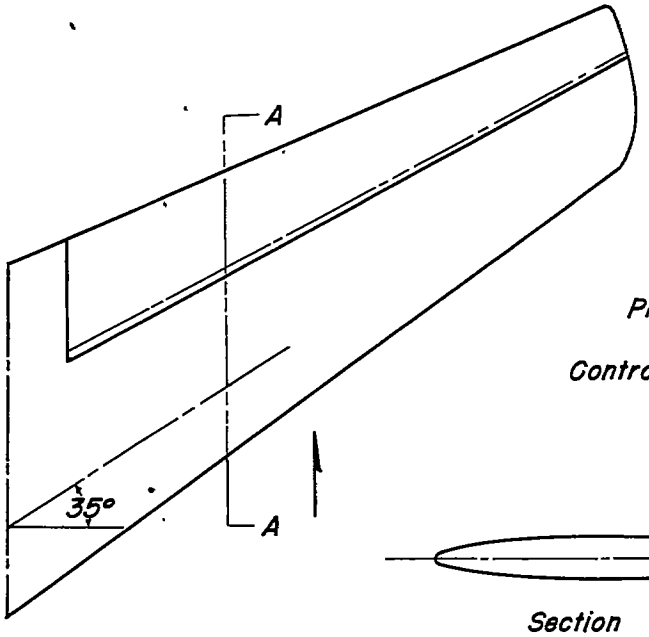

Planform

Control Surface G

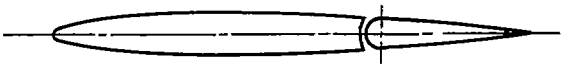

Section A–A

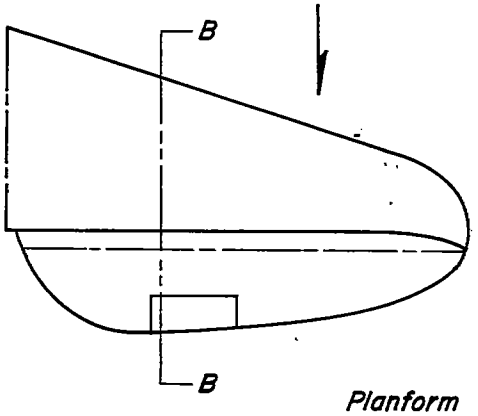

Planform

Control Surface H

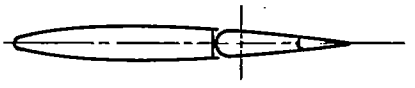

Section B–B

(c) Control Surfaces G and H.

Figure 1.— Continued.

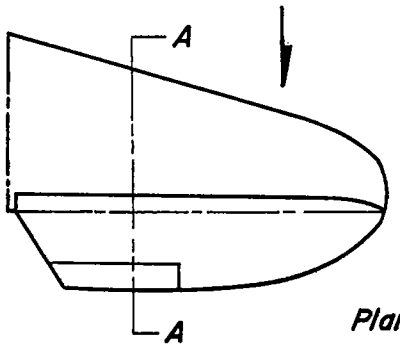

Planform

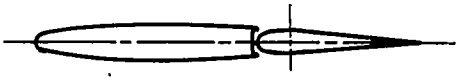

Section A–A

Control Surface I

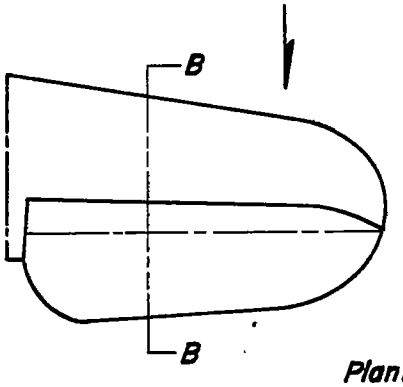

Planform

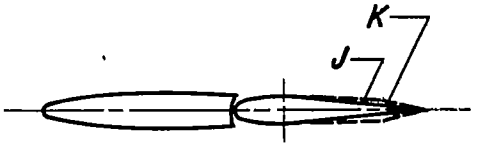

Section B–B

Control Surfaces J and K

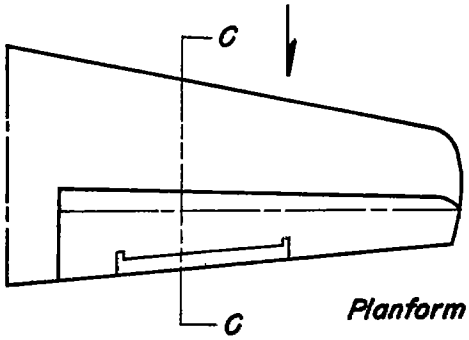

Planform

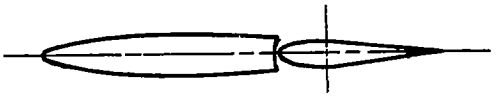

Section C–C

Control Surface L

(d) Control Surfaces I, J, K, and L.

Figure 1.—Continued.

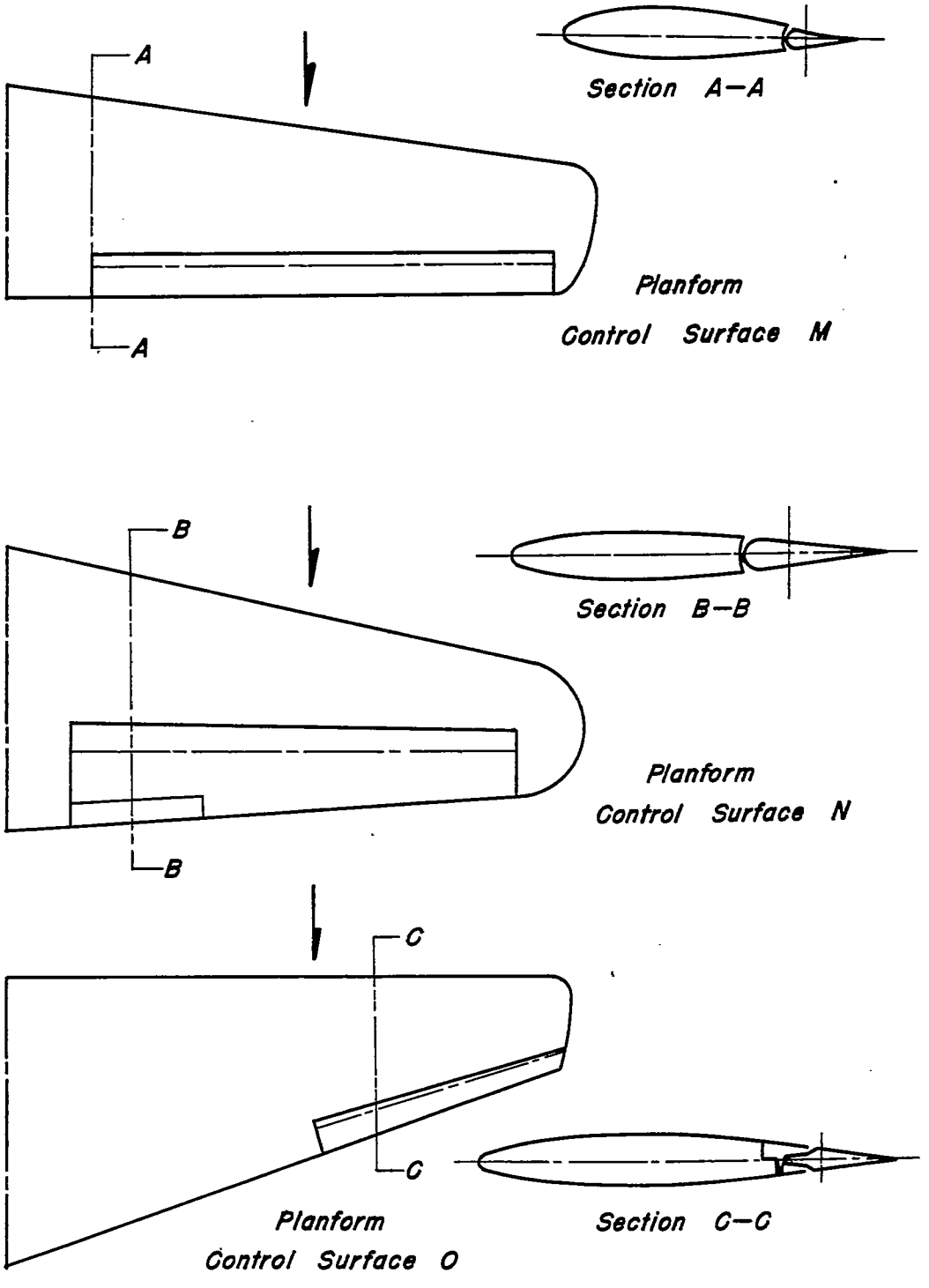

(e) Control Surfaces M, N, and O.

Figure 1. — Continued.

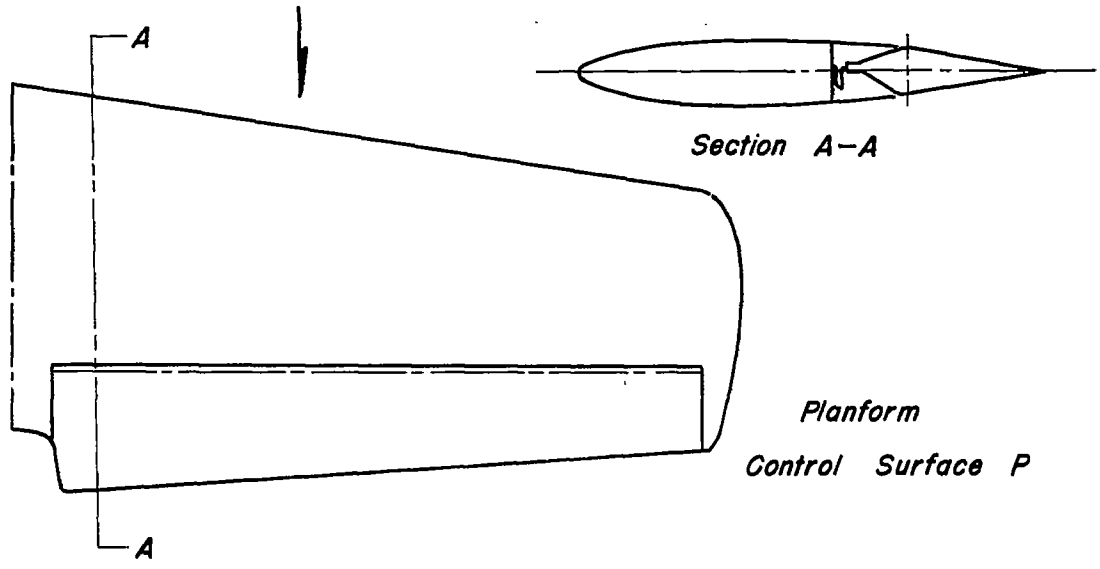

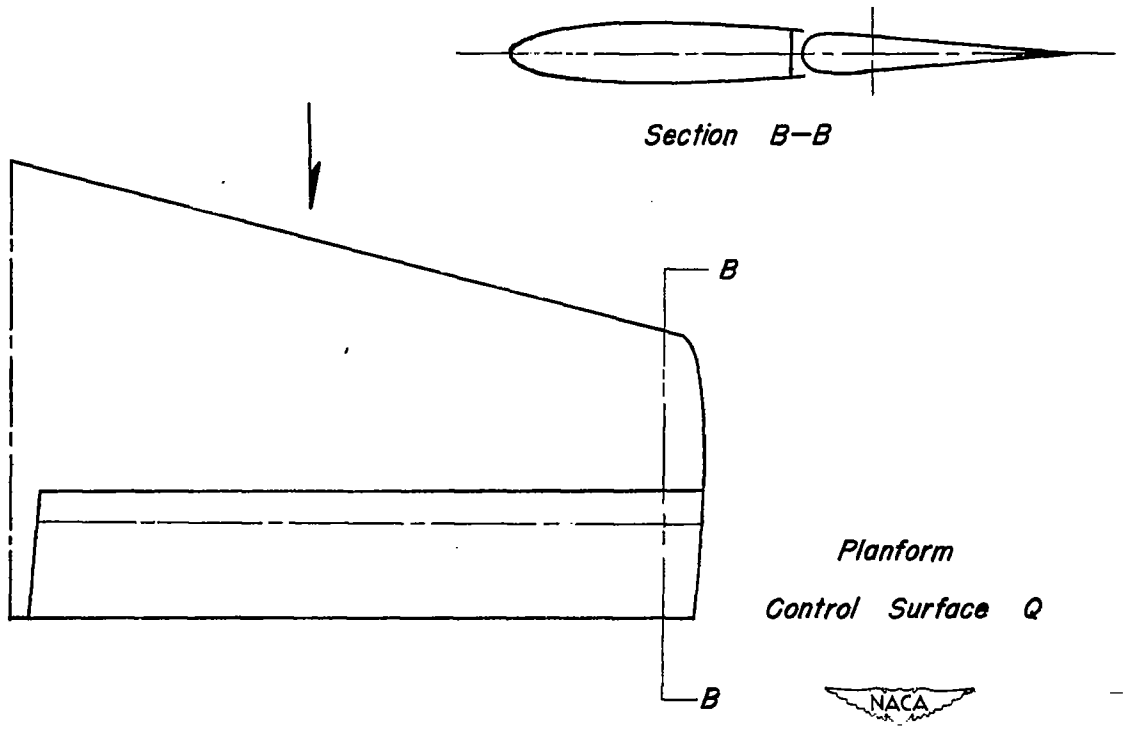

(f) Control Surfaces P and Q.

Figure 1. — Continued.

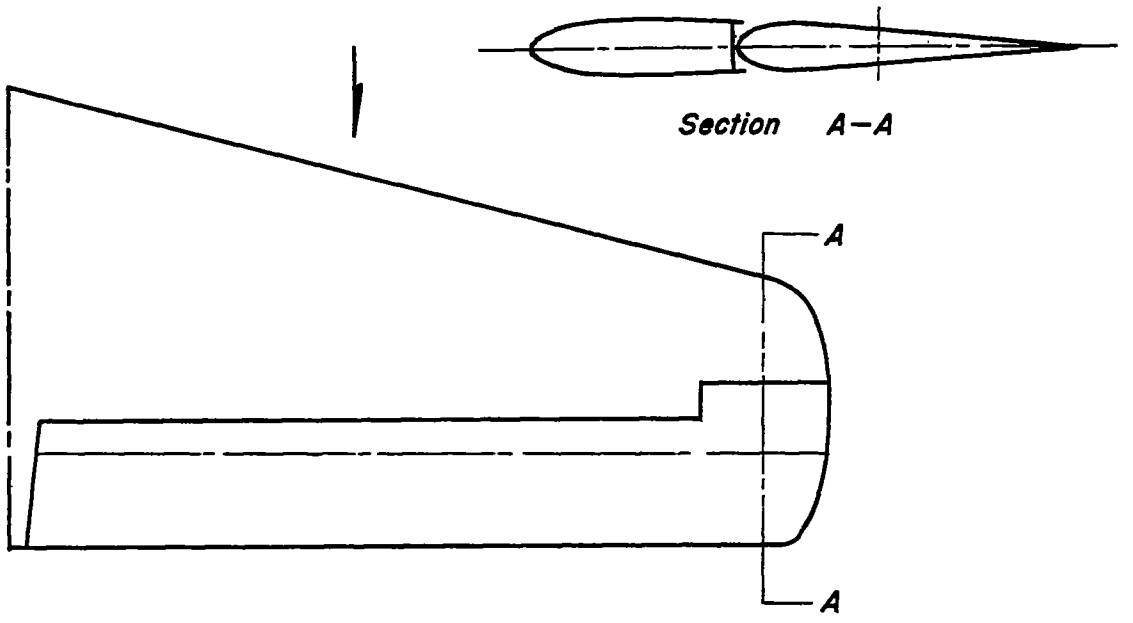

Planform

Control Surface R

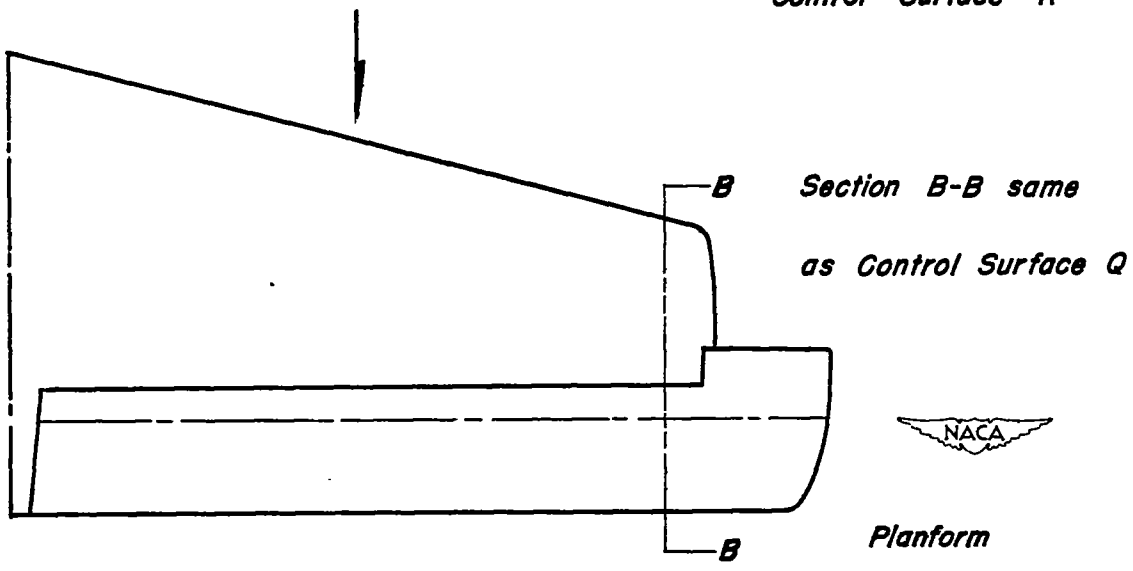

Section B-B same as Control Surface Q

Planform

Control Surface S

(g) Control Surfaces R and S.

Figure 1.– Continued.

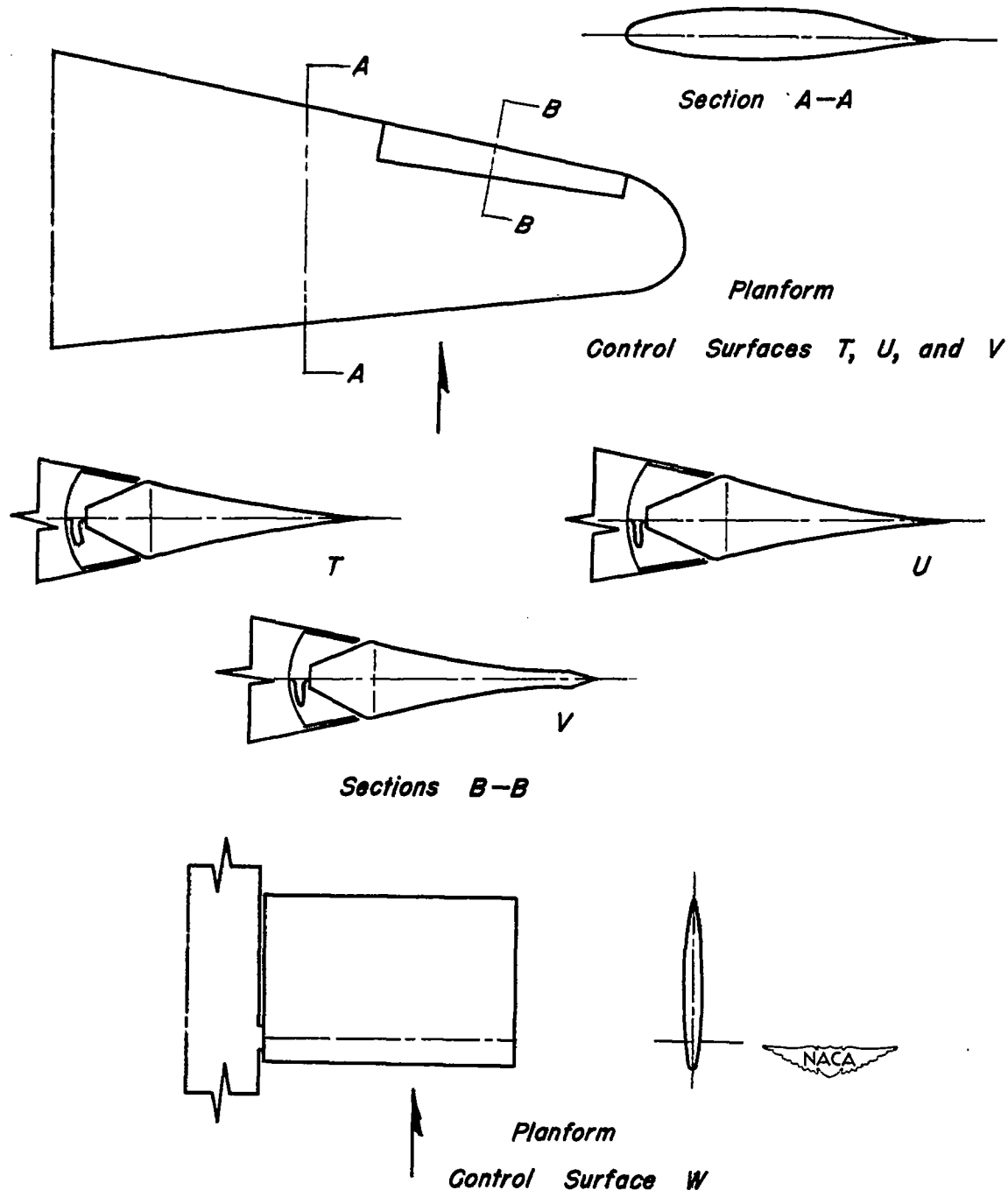

(h) Control Surfaces T, U, V, and W.

Figure 1.— Continued.

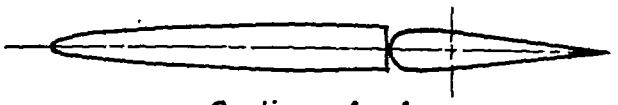

Section A—A

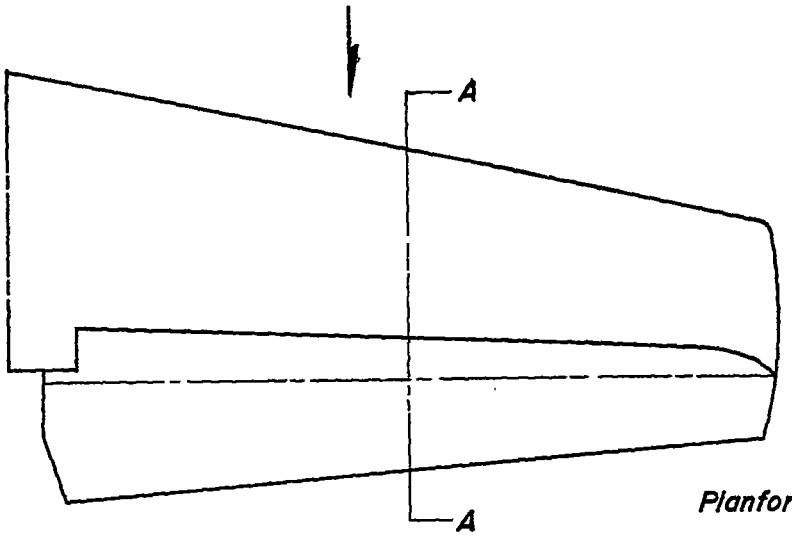

Planform

Control Surface X

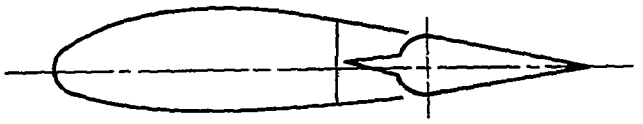

Section B—B

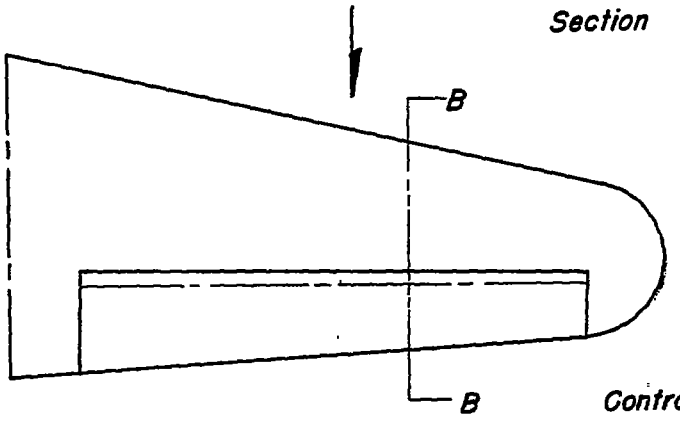

Planform

Control Surface Y

(i) Control Surfaces X and Y.

Figure I.—Concluded.

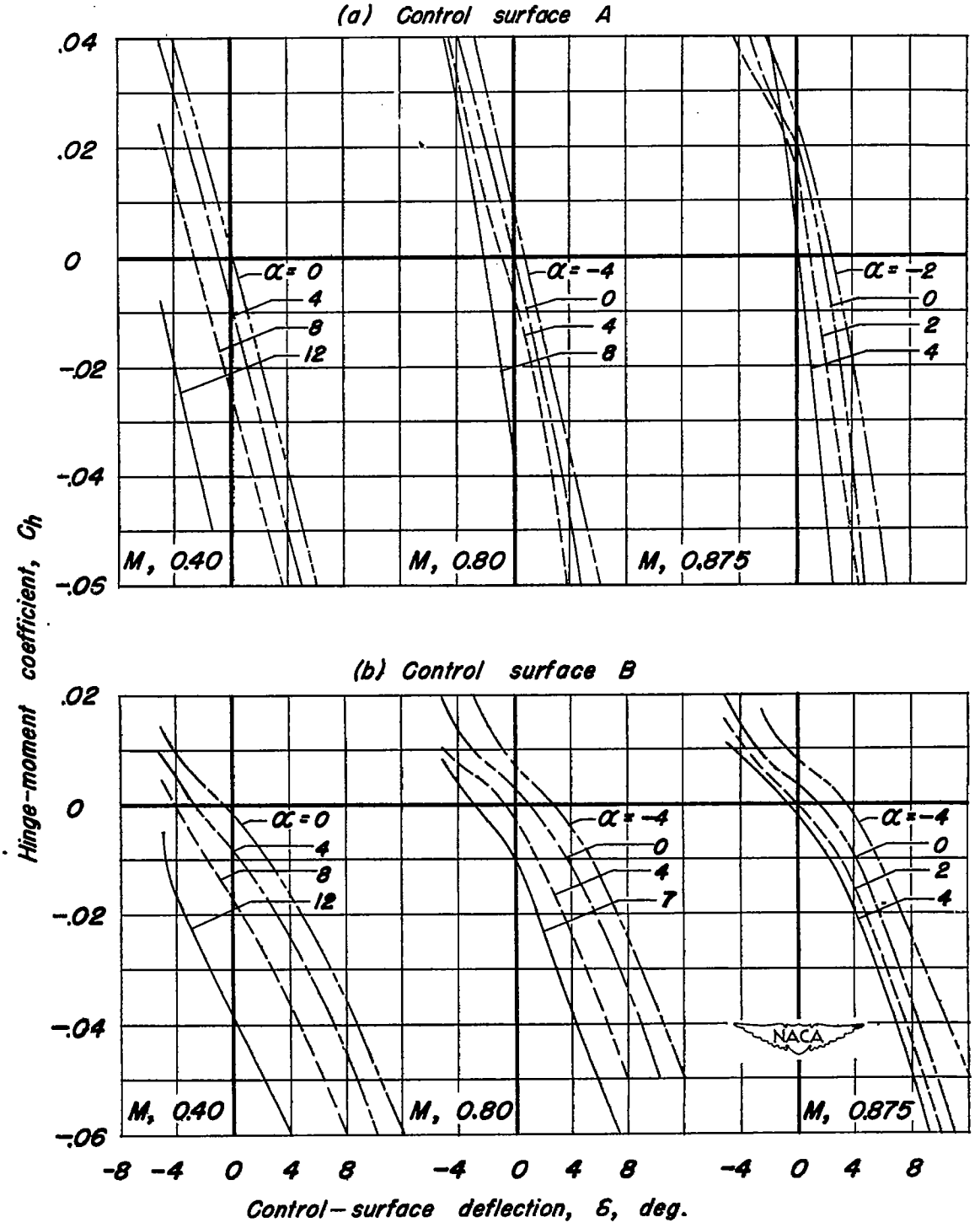

Figure 2. — Variation of hinge-moment coefficient with control-surface deflection.

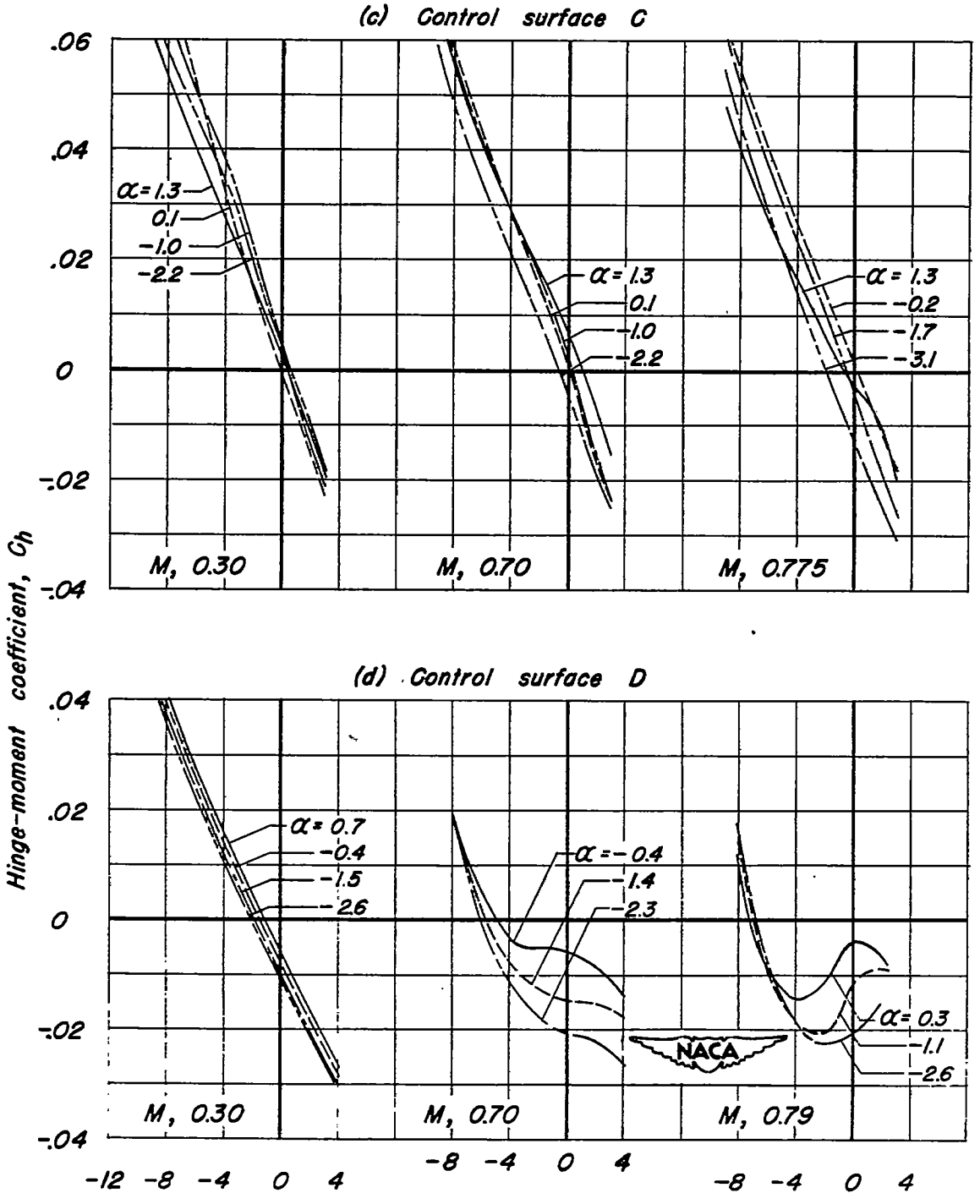

Figure 2. — Continued.

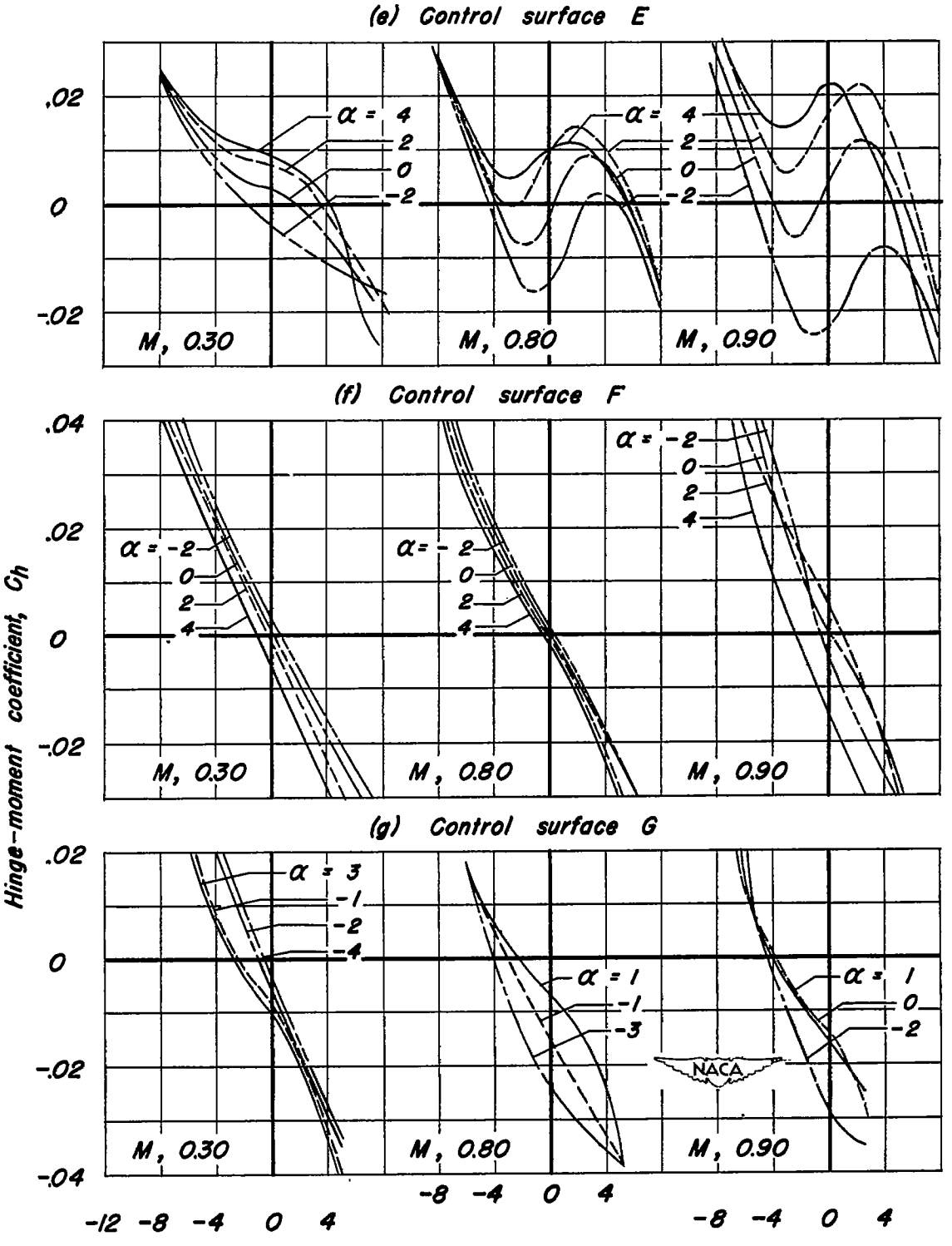

Figure 2. — Continued.

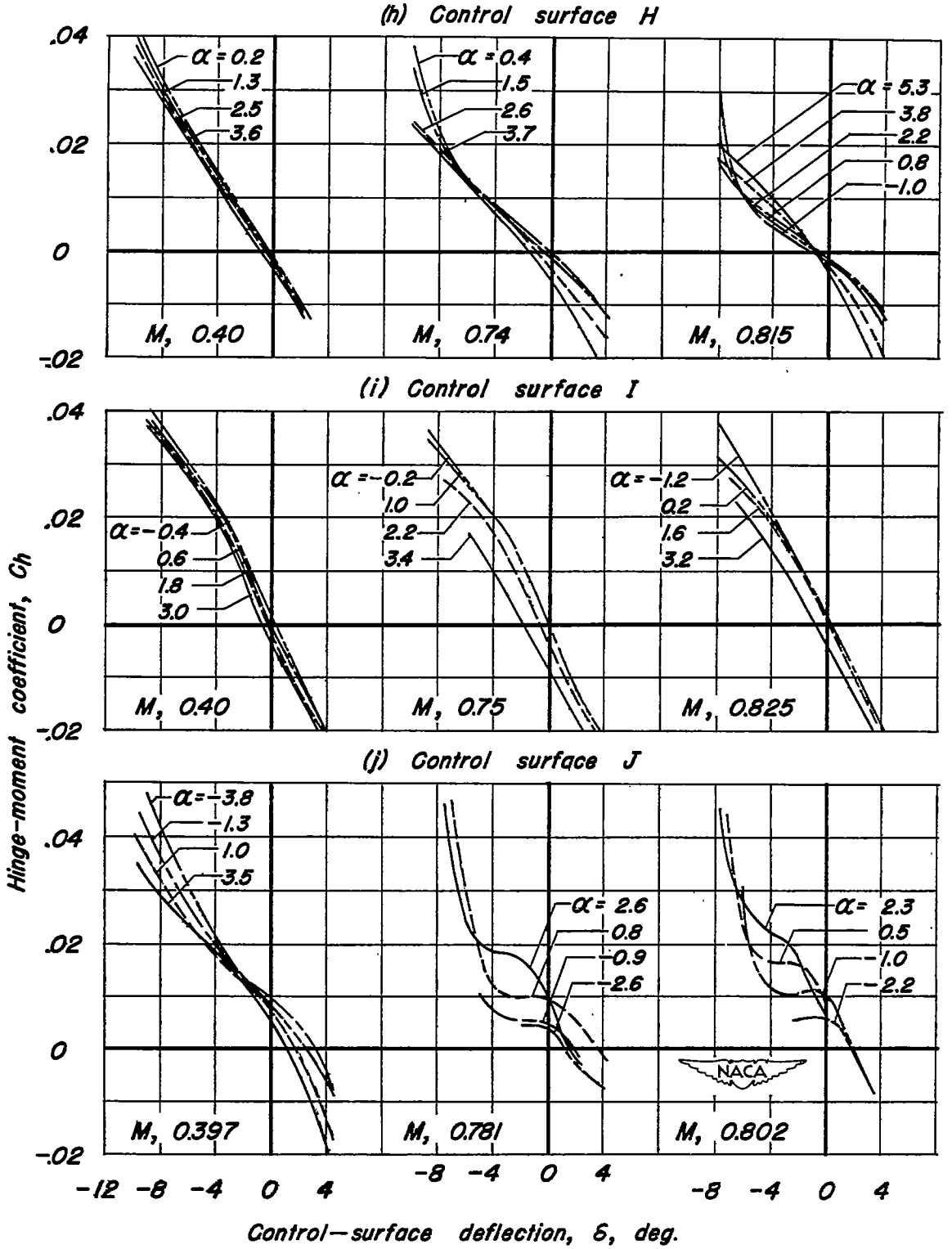

Figure 2.— Continued.

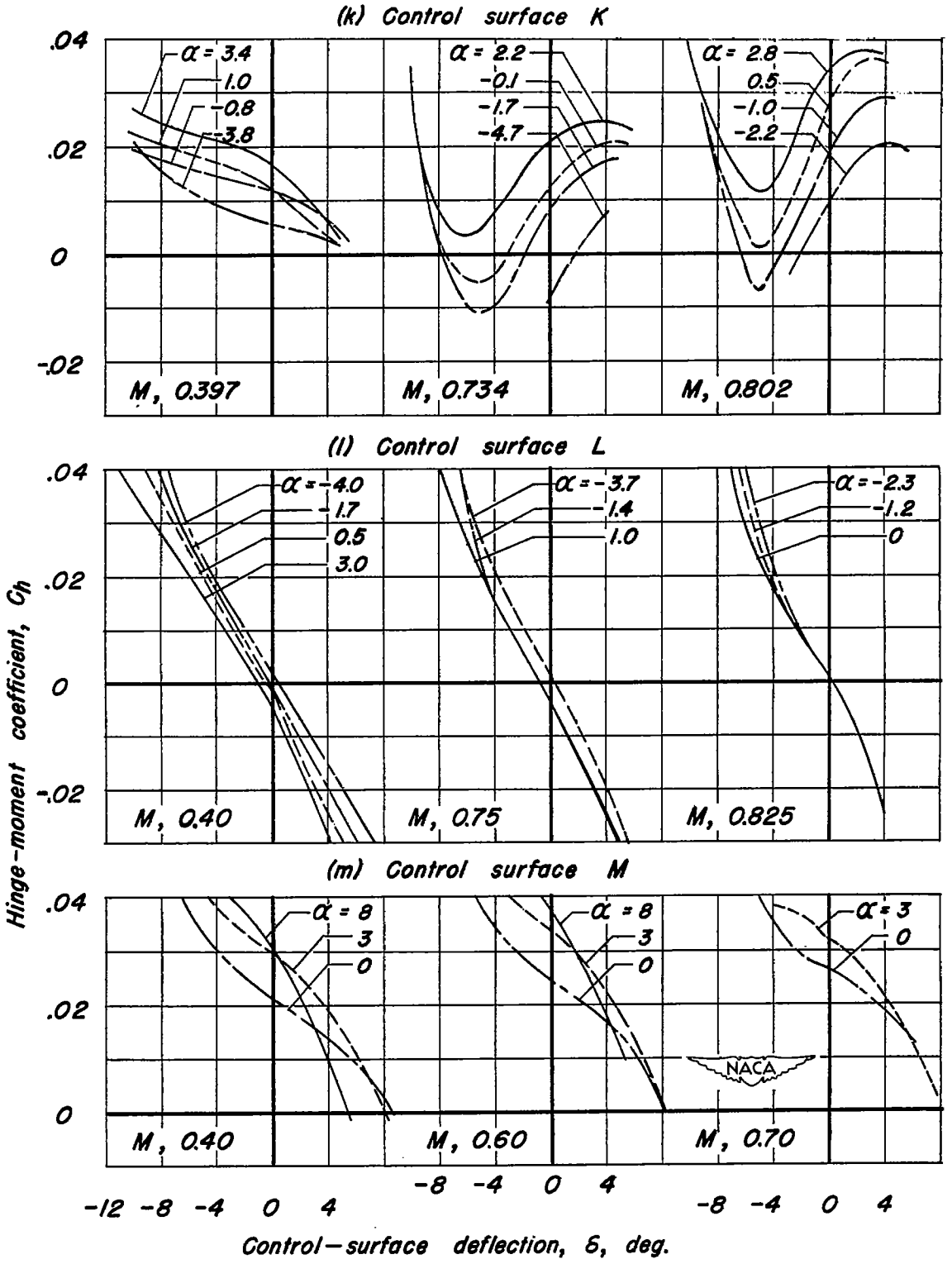

Figure 2. — Continued.

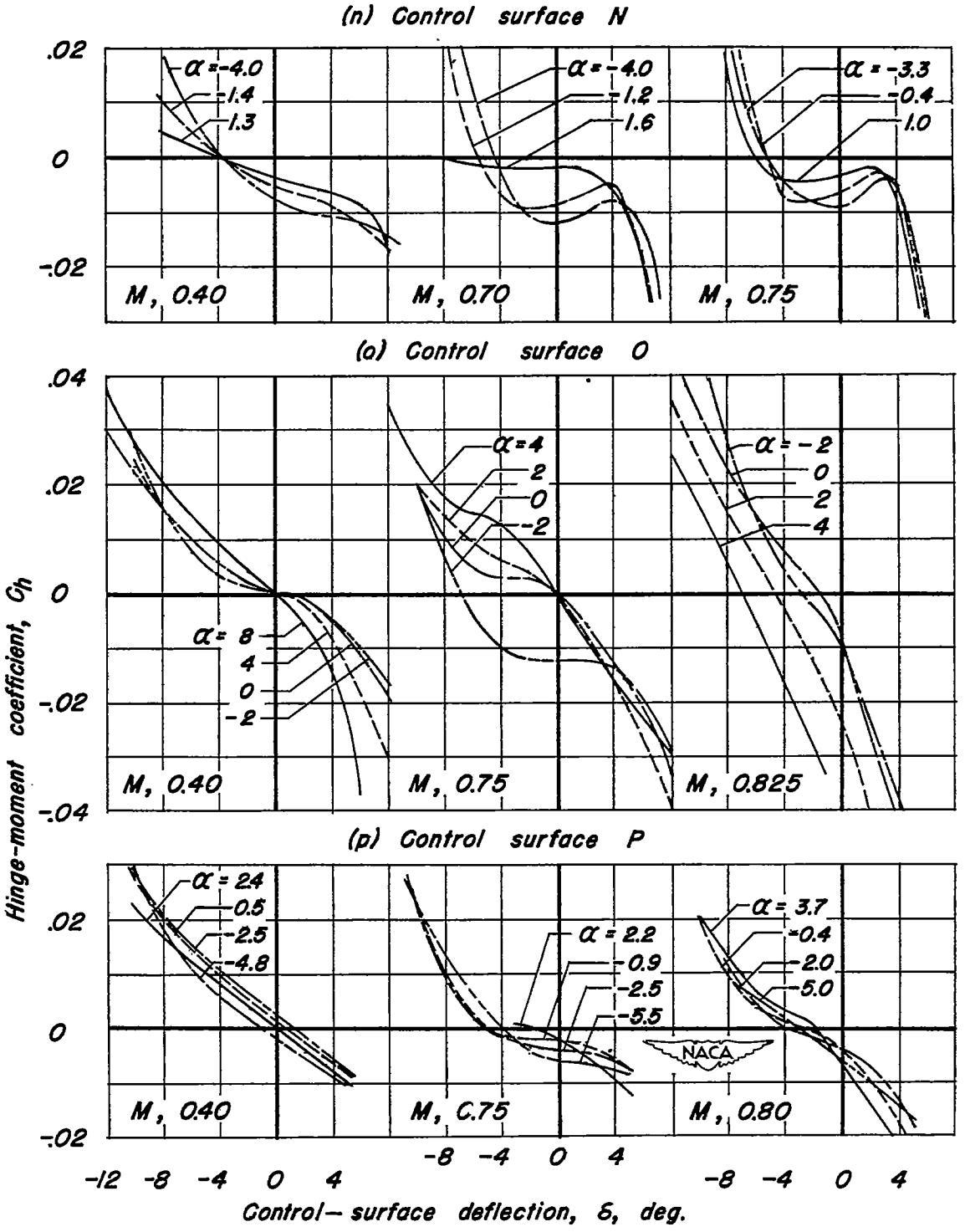

Figure 2.—Continued.

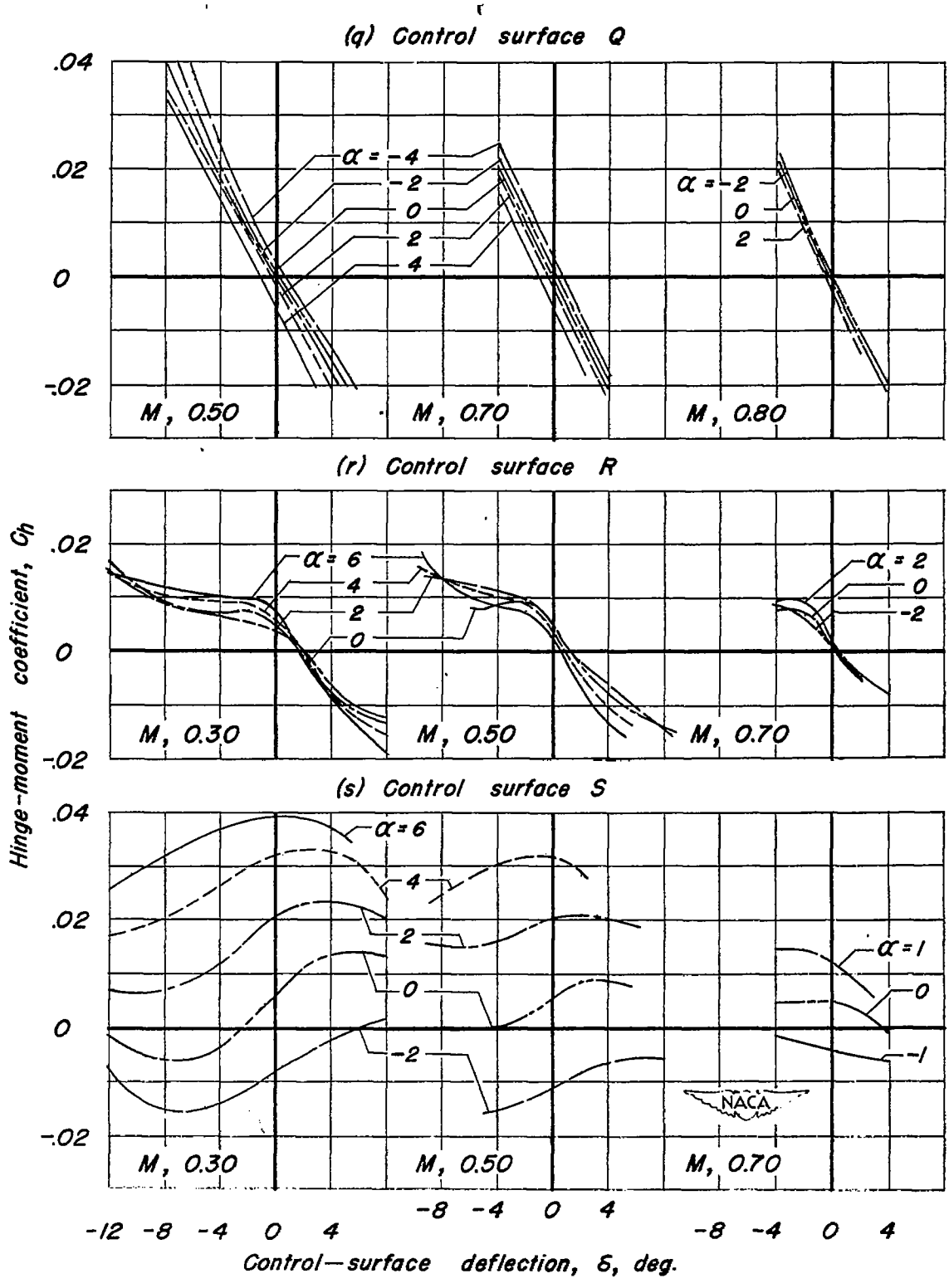

Figure 2.—Continued.

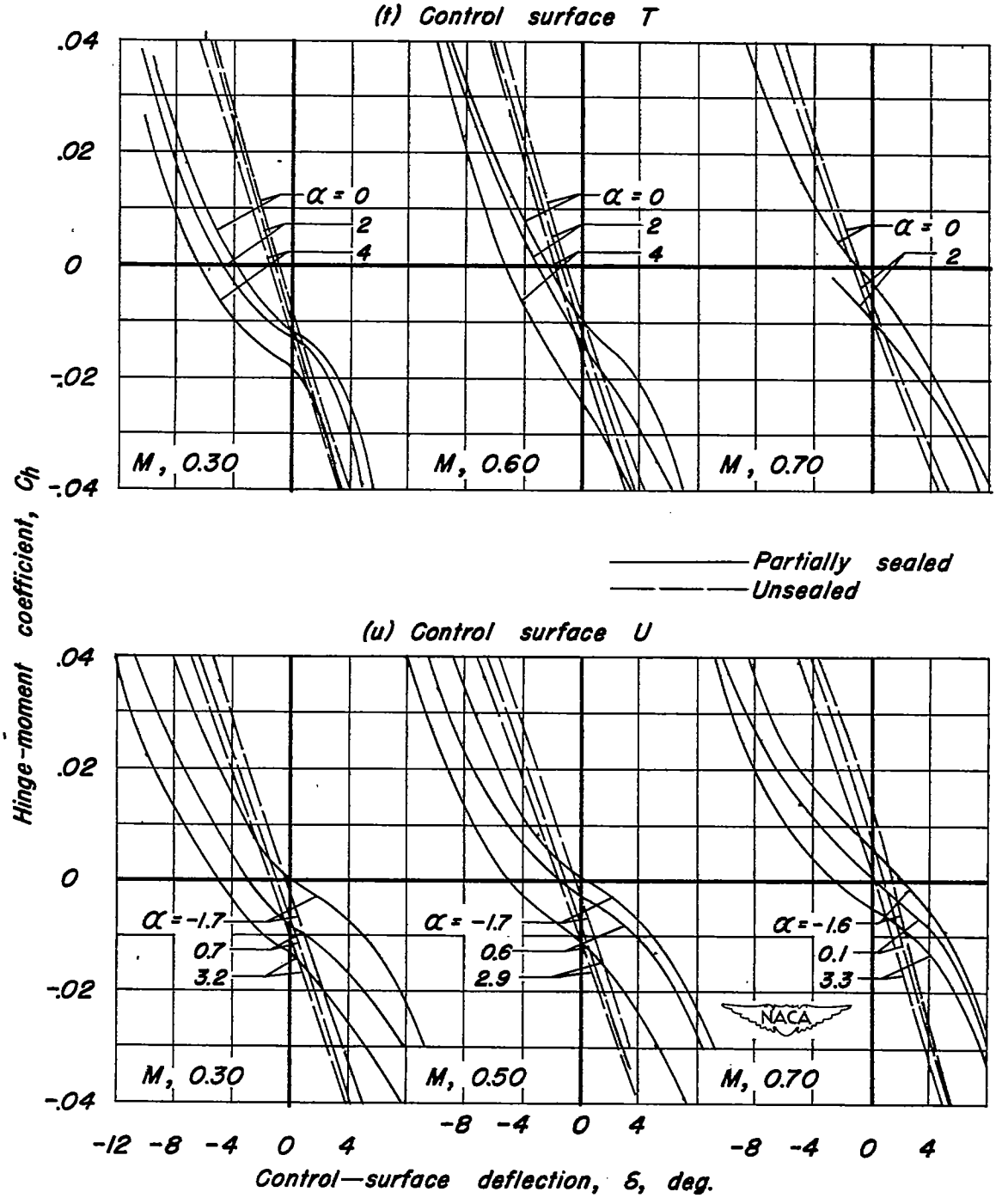

Figure 2.—Continued.

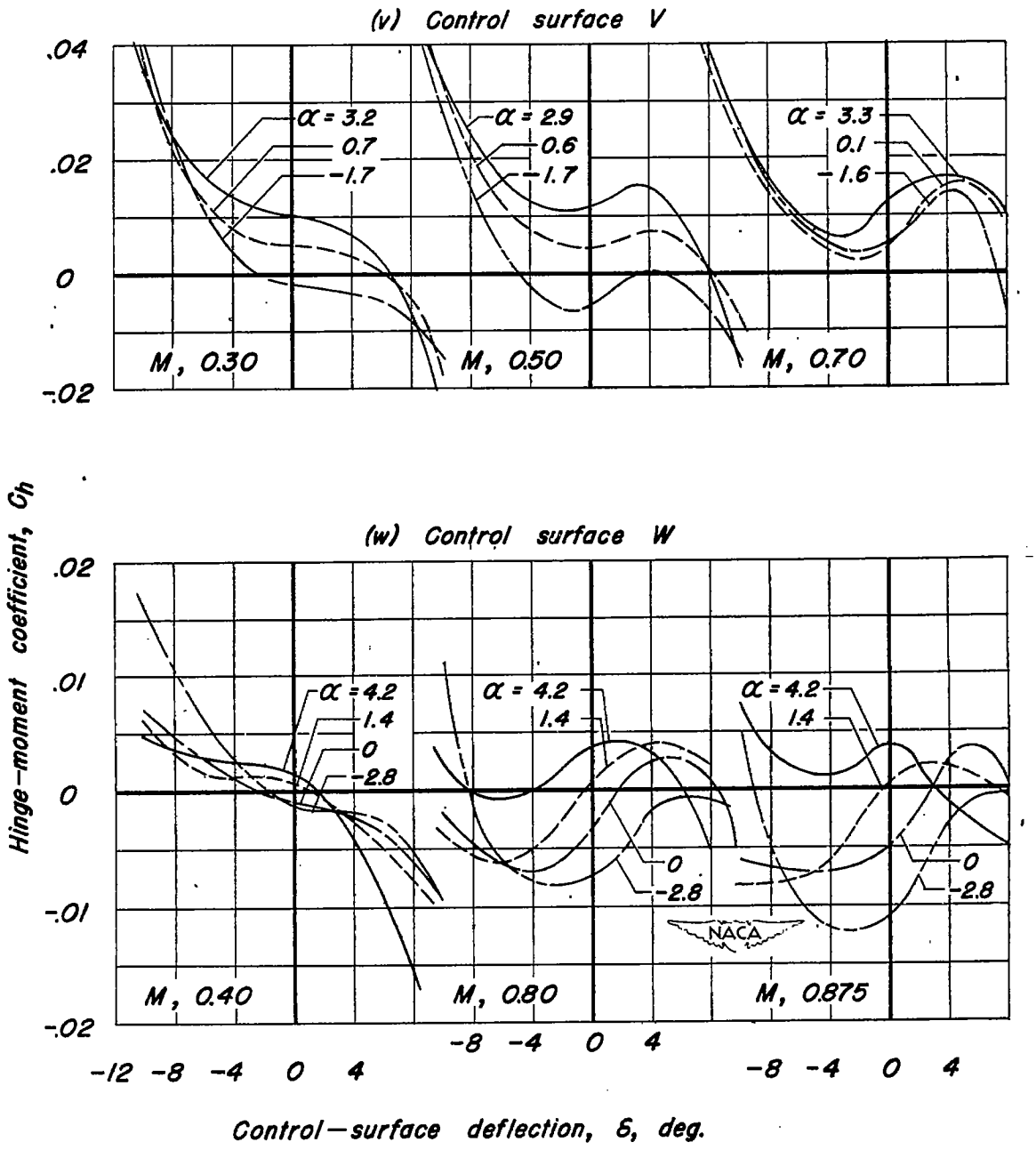

Figure 2. — Continued.

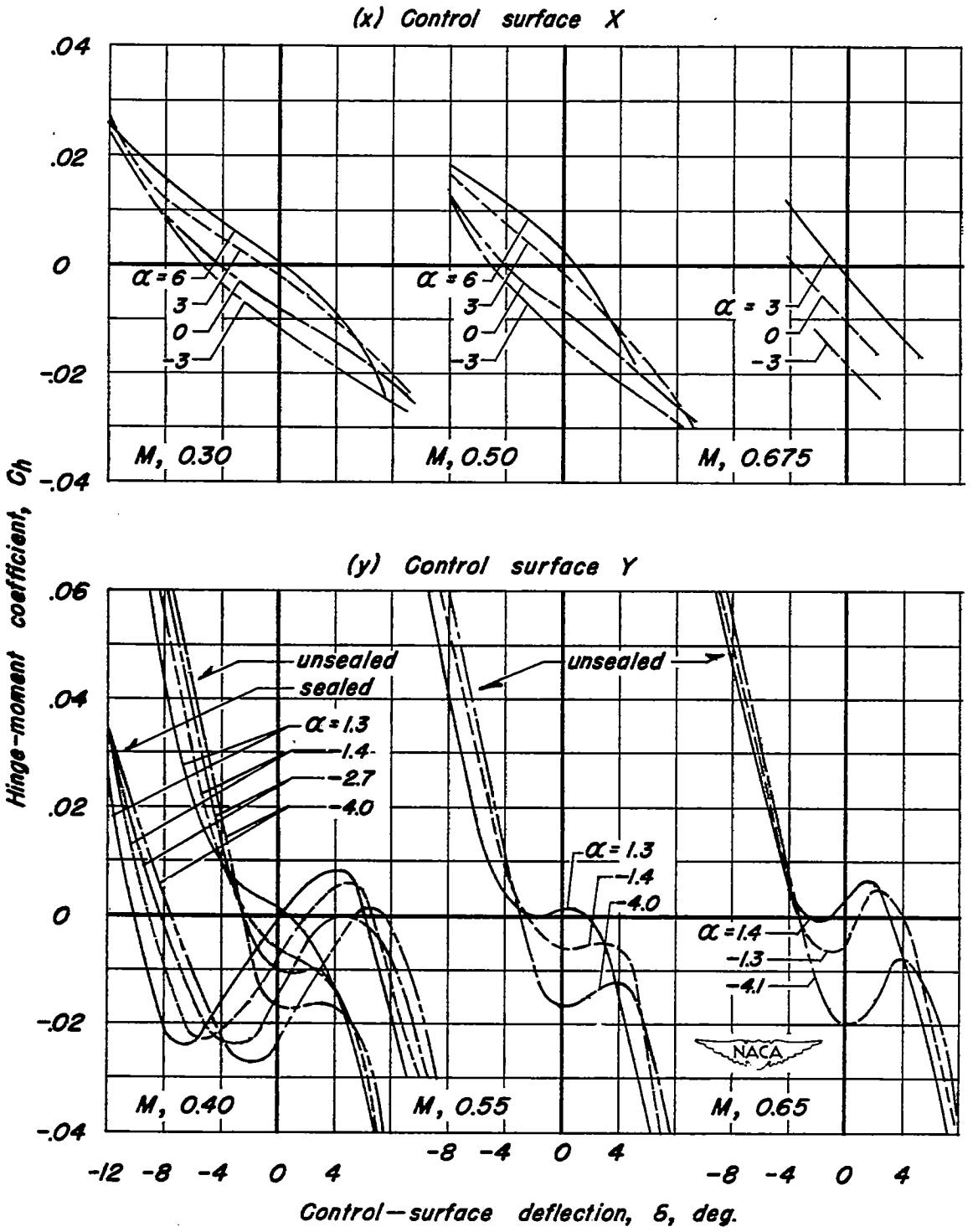

Figure 2.—Concluded.

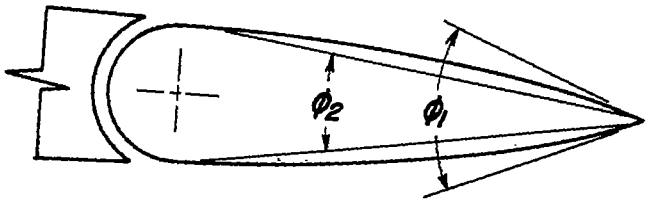

(a) Airfoil contour
(Convex)
$r > 1$

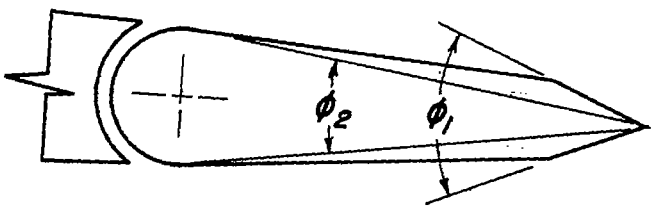

(b) Beveled trailing edge
$r > 1$

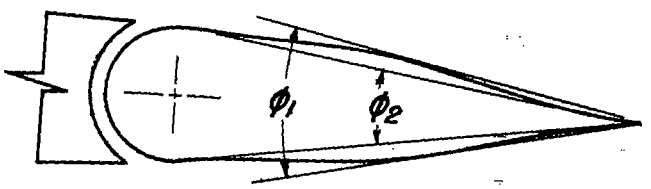

c Bulged contour
$r > 1$

(d) Airfoil contour
(Concave)
$r < 1$

Figure 3.— Measurement of angles ϕ_1 and ϕ_2 used in defining the control surface parameter r, the ratio ϕ_1/ϕ_2.

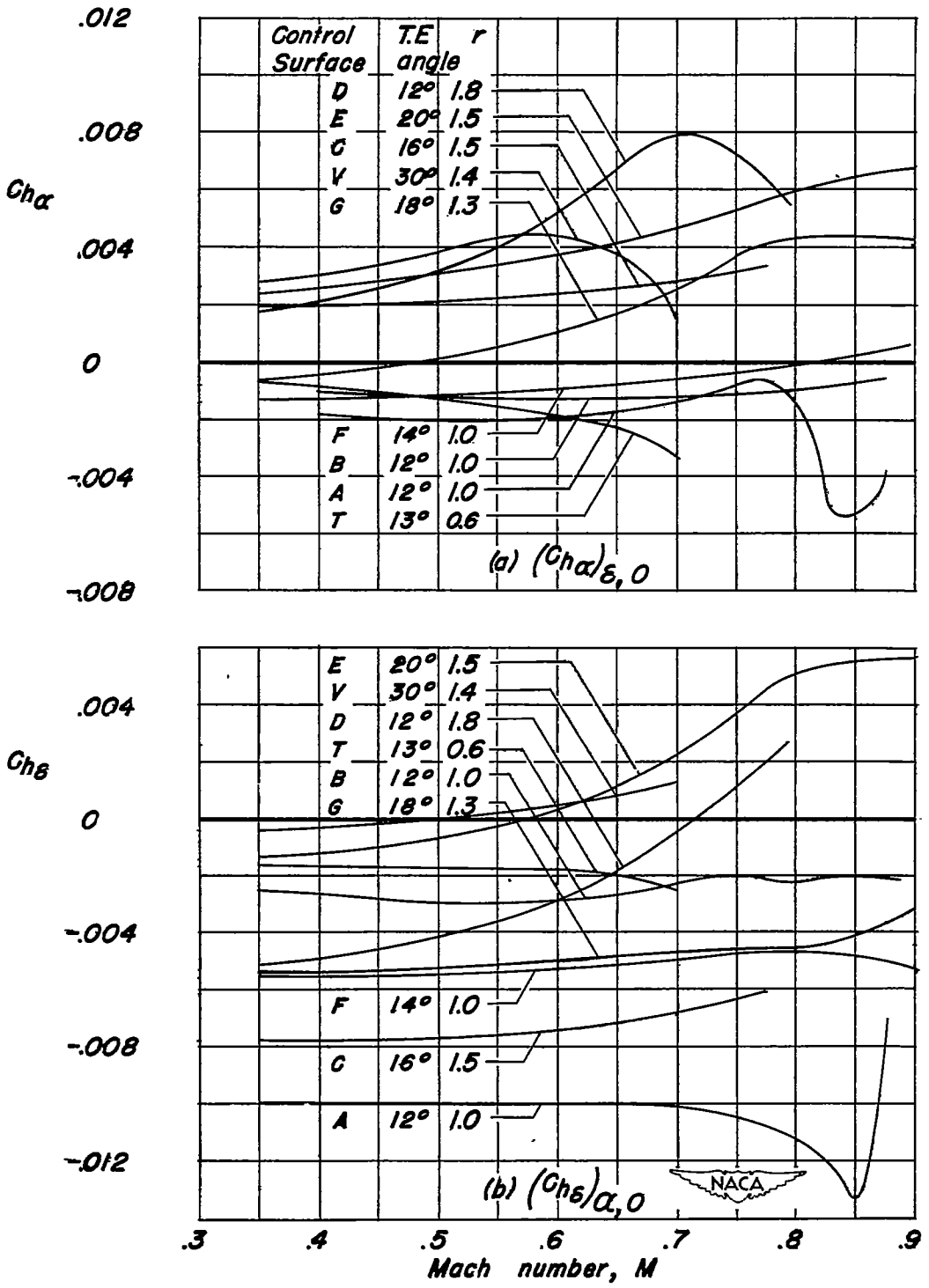

Figure 4.—Effect of control-surface profile aft of the hinge line on the variations of C_{h_α} and C_{h_δ} with Mach number.

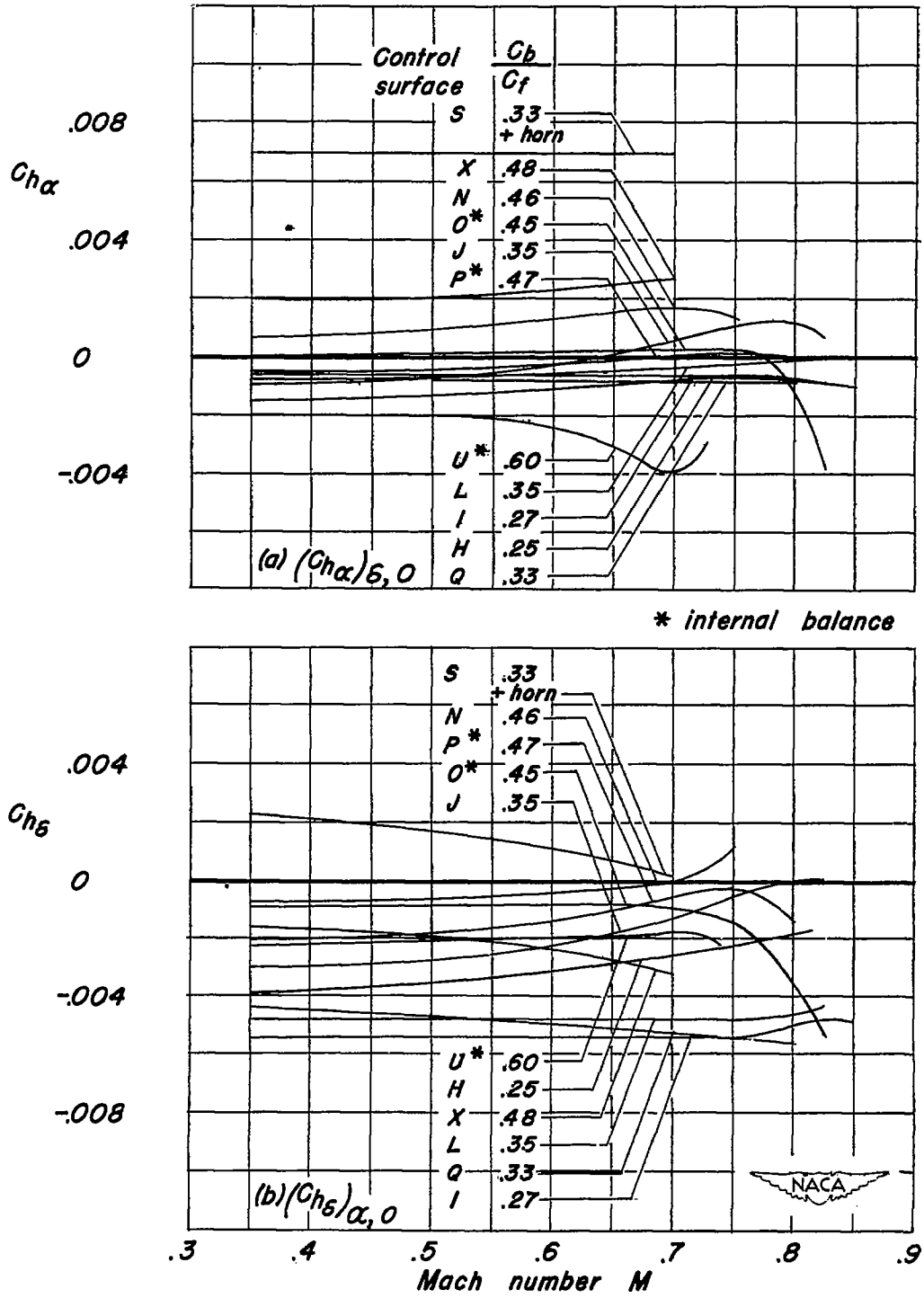

Figure 5.– Effect of aerodynamic nose balance on the variation of C_{h_α} and C_{h_δ} with Mach number.

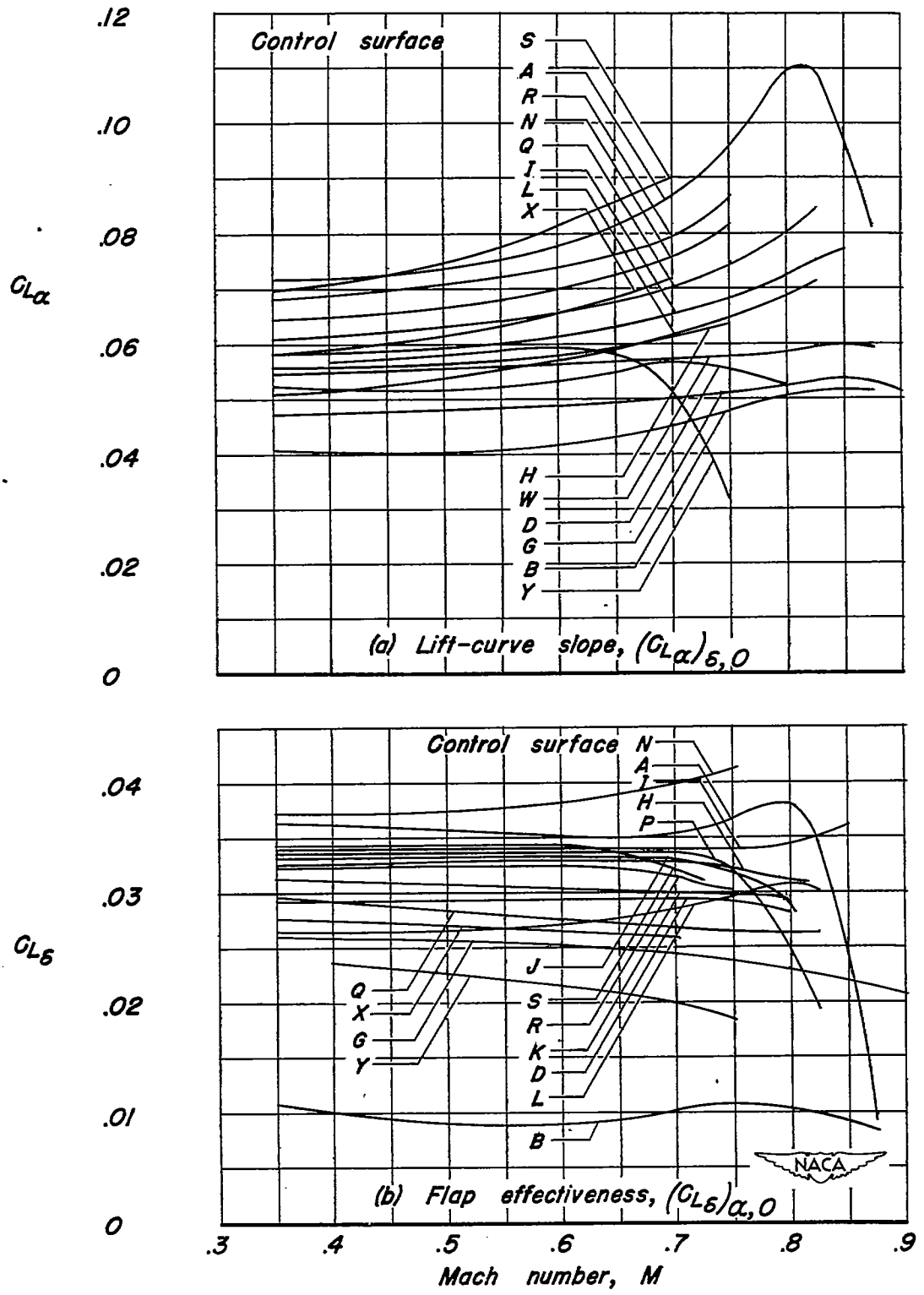

Figure 6.– Variation of lift-curve slope and flap effectiveness with Mach number.

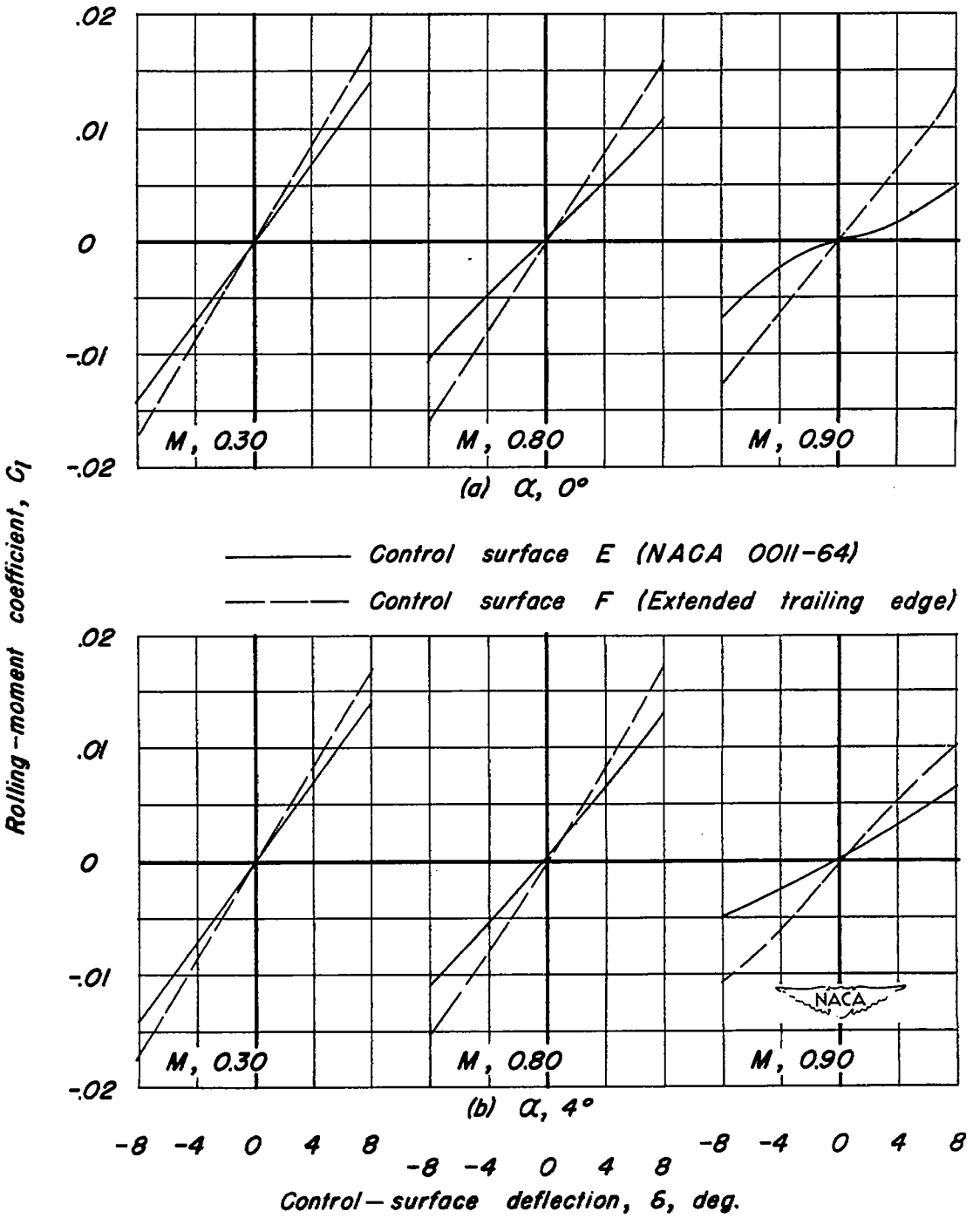

Figure 7.- Effect of trailing-edge profile on the rolling effectiveness of sweptback control surfaces E and F.

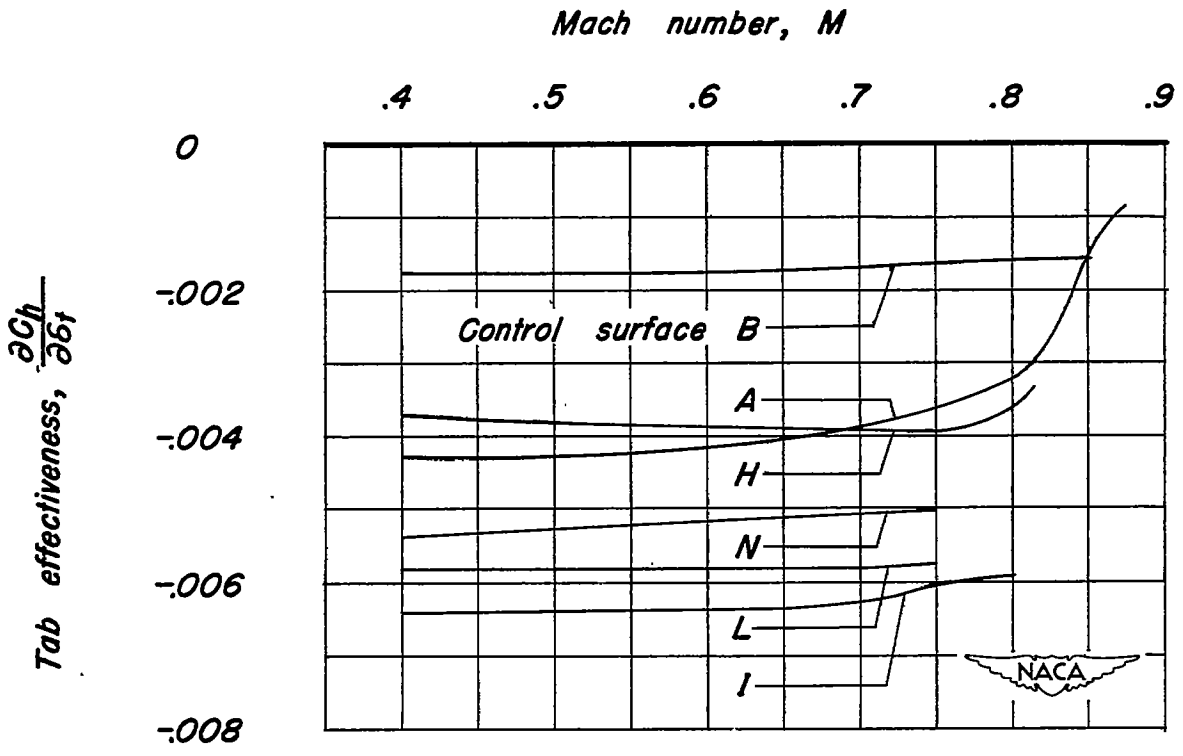

Control surface	$\frac{S_t}{S_f}$	$\frac{S_t\, l}{b_f\, \bar{c}_f^2}$
A,B	.031	.048
H	.066	.100
I	.138	.132
L	.098	.087
N	.127	.122

Figure 8.— Variation of tab effectiveness with Mach number. α, δ_f, 0°.